The Relationship between the Structure and Magnetic Properties of Bioinspired Iron(II/III) Complexes with Schiff-Base-Like Chelate Ligands, Part I: Complexes with Dianionic [N_4] Macrocycles

Birgit Weber[a][‡] Indira Käpplinger,[a] Helmar Görls,[a] and Ernst-G. Jäger*[a]

Keywords: Bioinorganic chemistry / Iron / Macrocycles / Magnetic properties / Schiff bases

The molecular structures and the spin ground-state of the iron(II/III) complexes **Fe1**, **Fe2** and **Fe3**, which contain dianionic macrocyclic [N_4] ligands derived from substituted acetylacetaldehydes and 1,2-diamines, have been investigated by X-ray analysis and temperature-dependent susceptibility measurements, respectively. The iron(II) complexes **Fe^{II}1** (which is dimeric by intermolecular coordination of one peripheral carbonyl group), **Fe^{II}1MeOH**, **$(Fe^{II}L)_2$dabco** (L = **1**, **2**, **3**; dabco = 1,4-diazabicyclo[2.2.2]octane) and the iron(III) complex **Fe^{III}1Cl** are pentacoordinate and have an intermediate-spin ground-state at room temperature (S = 1 for Fe^{II}; S = 3/2 for Fe^{III}). The intermediate-spin state was confirmed by DFT-MO calculations for **Fe^{II}1MeOH** and **Fe^{III}1Cl** and is also in agreement with the Mössbauer data of **Fe^{II}1** and ESR measurements of **Fe^{III}1Cl**. The iron centre in **Fe^{II}2** is nearly square-planar and shows a strong decrease of the magnetic moment below $T \approx 250$ K. This is probably due to an S = 0 to S = 1 spin-crossover or, more likely, to intermolecular antiferromagnetic interactions (shortest Fe–Fe distance of 3.4 Å). A new pair of octahedral iron(II/III) complexes with an N-heterocyclic axial ligand, **$Fe^{II}3(Py)_2$**/[**$Fe^{III}3(Py)_2$**]PF_6, could be crystallised. In contrast to the previously described pairs **$Fe^{II}1(Him)_2$**/[**$Fe^{III}1(Him)_2$**]PF_6 and **$Fe^{II}2Py_2$**/[**$Fe^{III}2Py_2$**]ClO_4, the orientation of the planes of the axial ligands is nearly independent of the oxidation step of the central atom. Octahedral derivatives with biologically relevant anions as axial ligands have been crystallised for the first time, namely [$BzEt_3N$][**$Fe^{III}1(NCS)_2$**], [Et_4N][**$Fe^{III}2(CN)_2$**]$(H_2O)_{0.5}$, Na[**$Fe^{III}2(NO_2)_2$**]$(MeOH)_2(H_2O)_{0.5}$ and [**$Fe^{III}2(NO_2)OH_2$**](MeOH). The latter shows a magnetic moment of $\mu_{eff} \approx 2.85\ \mu_B$ at room temperature, which decreases to 1.85 μ_B at lower temperature. This indicates an incomplete S = 1/2 to S = 3/2 spin-crossover, which is probably due to the presence of H_2O as a weak axial ligand.

Introduction

Iron is known to be a ubiquitous biometal with a great variety of metabolic functions.[1] Many iron-containing proteins are derived from haem with the porphyrinato macrocycle as a typical dianionic equatorial [N_4] ligand. The unique biological role of (porphyrin)iron compounds may be one reason for the unbroken interest in this important class of molecules over nearly a century. This is reflected in the countless number of papers and many extensive reviews, monographs and handbooks.[2] Compared with the porphyrins, including such variations as expanded porphyrins, confused porphyrins etc., there are only a few other examples of similar [N_4] macrocycles that can act as dianionic equatorial ligands. Besides the synthetic porphyrins and their tetrabenzotetraaza derivatives, the phthalocyanines and complexes with tetradentate [N_2O_2]-coordinated dianions of *N*,*N*-bridged salicylaldimines (e.g. "salen") have been investigated extensively, and in part quite successfully, as models for the active sites of haem proteins. For instance, the reversible uptake of dioxygen − the main function of haemoglobin − was realized with simple "(salen)Co" much earlier[3] than with (porphyrin)iron compounds detached from the protein; the first catalysts of technical relevance for cytochrome-P450-like oxygenation reactions were derived from (salen)Mn.[4]

During the last decades we have created a pool of chelate complexes[5] with ligand systems that can be subdivided into the three basic structures given in Scheme 1. All these compounds are structural or functional models of active sites of metalloenzymes: Type **I**, which is formally most related to porphyrins, contains tetradentate twofold negatively charged macrocyclic ligands with an [N_4] donor set and a more or less extended π-system. [The special ligand Me_4TAA, first published in 1969 as its nickel complex (Me_4TAA)Ni[6] and today known in complexes with nearly all transition elements and many main group metals,[7] has been characterised by F. A. Cotton: "The latter bears many similarities to porphyrinato systems, but its chemical behav-

[a] Institute of Inorganic and Analytical Chemistry, University of Jena,
August-Bebel-Strasse 2, 07743 Jena, Germany
Fax: +49-3641-442716
E-mail:cej@uni-jena.de.
[‡] Present address: Ludwig-Maximilians-Universität München, Department Chemie,
Butenandtstraße 5–13 (Haus D), 81377 München, Germany

 DOI: 10.1002/ejic.200400759

iour seems to be even more diverse."[7b]] Type **II** is derived from dianionic open-chain ligands with an [N_2O_2] coordination sphere ("salen" is a special case with a fused benzene ring for $R^1 + R^2$). Type **III** is derived from tridentate dianions; the coordinatively highly unsaturated formula unit promotes the formation of oligonuclear structures[8] similar to those found in biological systems. Previous investigations on cobalt, copper and nickel complexes of types **I**, **II** and **III** have already shown that the variation of the *N*,*N*′-bridges X, Y and the substituents R^{1-3} can be used to control properties such as the electronic state of the central atom,[9] the redox potentials,[10,11a,11d,11e] the affinity of vacant axial coordination sites towards additional ligands,[11] as well as the binding and activation of dioxygen,[5b,12] carbon dioxide[13] or nitric oxide.[14] These results indicated that the macrocycles **I** and, in some respect, also the complexes **II** share many common characteristics with porphyrins, but marginal ligand variations can dramatically change the behaviour. This situation is particularly typical of the chemistry of the iron complexes.

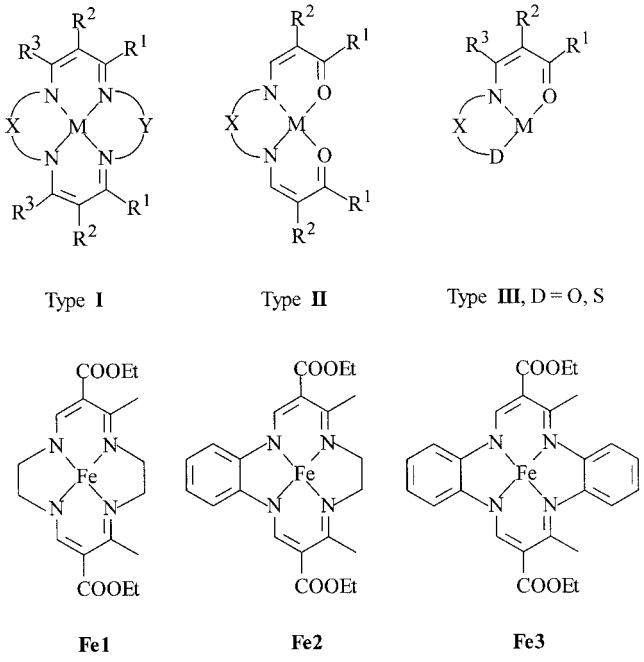

Scheme 1. Formulae of basic chelate complexes studied in our laboratory (**I**–**III**) and formulae of macrocyclic iron complexes used in this work (**Fe1**–**Fe3**). The arabic numbers represent the dianion of the macrocyclic ligand $\mathbf{H_2L}$ ($\mathbf{L^{2-}}$ = **1**, **2**, **3**). **Fe1a** denotes the more hydrophilic variant of **Fe1** with acetyl (COMe) instead of the ester groups COOEt. The abbreviation $\mathbf{Me_4TAA}$ ("tetramethyldibenzo*tetraaza*[14]*annulene*") is used for $\mathbf{L^{2-}}$ in type **I** with X = Y = *o*-phenylene, $R^1 = R^3$ = Me, and R^2 = H. The basic macrocycles **FeL** and the axial ligands [MeOH, dabco (μ-1,4-diazabicyclo[2.2.2]-octane), Py (pyridine), N-MeIm (*N*-methylimidazole), I^- etc.] are given in bold (with the exception of the tables); all other components of the formula units or within the lattice are given in plain characters.

Busch et al.,[15a,15b] Holm et al.[15c,15d] and Goedken et al.[16] have described iron(II/III) complexes of type **I** with R^2 = H or Ph. The parent compound of **Fe1** (R^2 = H) has been characterised as a square-planar intermediate-spin (S = 1) complex[15a] that gives an octahedral diadduct, probably with a high-spin (S = 2) ground state, in pyridine solution. No addition of imidazole − a very characteristic reaction of (porphyrin)iron compounds − could be observed. Even in our earlier reports[17] we accentuated the high tendency of the carbonyl-substituted derivative **Fe1** to give octahedral low-spin diadducts, especially with imidazole. Many such derivatives have been isolated as solids and could be characterised by X-ray structure analysis and susceptibility measurements.[18] The existence of others (also with biologically relevant anions such as nitrite and sulfite[19b]) could be proved in solution by spectrophotometric titration.[19] In this respect, the carbonyl-substituted derivative **Fe1** is more closely related to porphyrins than the parent compound. On the other hand, several pentacoordinate iron(III) halides of type **I** have been described as intermediate-spin (S = 3/2) complexes,[15,20] whereas the derivative $\mathbf{Fe(Me_4TAA)Cl}$ has a high-spin (S = 5/2) ground state, just as most halides of (porphyrin)iron(III) compounds. The formation of various pentacoordinate halides and pseudo-halides **Fe1X** (X = F, Cl, Br, I, N_3^-, SCN^-) has been monitored by spectrophotometric equilibrium studies in two-phase systems,[21] but their spin state is uncertain in some cases. In contrast, all the pentacoordinate nitrosyl derivatives **FeLNO** (**L** = **1**, **2**, **3**) have an S = 1/2 ground state, just as the analogous (porphyrin)iron compounds.[22]

The existence of coordinatively unsaturated species that are able to reversibly bind additional axial ligands, as well as the possibilities of changing the oxidation number and the spin state of the central atom, are key features of many haem proteins. For instance, the iron(II) atom in deoxygenated haemoglobin has an effective coordination number of five as the bonding to the nitrogen atom of the imidazole ring of the "proximal" histidine group causes a strong displacement from the [N_4] plane of the equatorial porphyrin; the ground state is high spin (S = 2). After oxygenation, the central atom is best described as six-coordinate low-spin (S = 1/2) iron(III) in a weakly distorted octahedral environment, antiferromagnetically coupled with the unpaired electron of an axially coordinated superoxide radical ion. For comparison with our macrocycles we are therefore mainly interested in structural and magnetic information as a function of the coordination number and the oxidation state of iron in these complexes.

This paper is focused on (i) the spin state of complexes with coordination number less than 6, (ii) the dependence of the orientation of axial N-heterocycles in octahedral diadducts on the oxidation state of the central atom, and (iii) attempts to isolate adducts with biologically relevant anions as solids for structural and magnetic studies.

Results and Discussion

Syntheses and General Characterisation

In contrast to the analogous nickel and copper compounds, the iron complexes of type **I** cannot be synthesised

by a direct metal-templated condensation of the precursor complexes of type **II** with diamines. The best synthetic method is the reaction of an iron(II) salt, chiefly the acetate, with the free ligands $\mathbf{H_2 1}$, $\mathbf{H_2 2}$ and $\mathbf{H_2 3}$, respectively, which can be obtained by demetallation of the copper(II) complexes. The synthesis of the basic iron(II) complexes **Fe1**,[17b,17c,21] **Fe2**[10d] and **Fe3**[23] has been described previously. However, since all these publications are in German in mainly non-international, and in part no longer available, journals, and also because some steps of the ligand syntheses have been modified to prevent the use of gaseous hydrogen sulfide, we will give a summary of the syntheses in the Experimental Section.

Adducts of the iron(II) complexes with axial ligands were obtained by adding an excess of the corresponding ligand to the reaction mixture during the synthesis of the iron(II) complex. The products precipitated upon slow cooling of the reaction mixture. In some cases mono- and/or diadducts were formed depending on the concentrations and the temperature regime.[17b,17c] Diffusion procedures are better suited for diadduct formation starting from the isolated parent complexes. The air sensitivity of the iron(II) complexes is strongly dependent on the type of additional axial ligands and decreases in general from **Fe1** to **Fe3**. This sequence is in agreement with the redox potentials of the complexes.[5c,10d]

The iron(III) complexes are best prepared starting from the iron(II) derivatives by in-situ oxidation with iodine in the presence of an excess of sodium iodide to promote the precipitation of the iodide **FeLI**.[20,21] The latter is a good precursor for a large range of iron(III) derivatives with different axial ligands.[5c,18] Carbon tetrachloride is a suitable Cl donor to yield the chloride derivatives **FeLCl**. All the iron(III) complexes are relatively air-stable but water-sensitive, especially in the presence of primary or secondary amines (piperidine!) or phosphonic acid esters as axial ligands. Here, hydrolysis and/or radical redox processes occur. All complexes are therefore best handled under dry argon.

Intermediate-Spin Complexes with Coordination Numbers 4, 4+1 and 5

Crystals suitable for X-ray structure analysis were obtained for the solvent-free iron(II) complexes **Fe1** and **Fe2**. Only one stable solvate with an O-donor, **Fe1MeOH**, could be crystallised. The previously described crystalline 1:1 solvates of **Fe1** with the N-donors ammonia or pyridine[17b] decompose even at room temperature under dry argon. Attempts were made with the alternative N-donor 1,4-diazabicyclo[2.2.2]octane (dabco) and, in all cases, good crystals

Table 1. Spin state (*S*), room-temperature magnetic moment (μ_{eff}) and bond lengths [Å] and angles [°] within the first coordination sphere of macrocyclic iron(II/III) complexes with coordination numbers (*CN*) 4, 4+1 and 5.

Complex	*CN*	*S* μ_{eff} [μ_B]	Fe–$N_{1,2}$[a]	Fe–$N_{3,4}$[a]	Average L_{eq}	Fe–L_{ax}	Fe–pl_{eq}[b]	Average N–Fe–N[c]	Average N–Fe–N[d]	Shortest Fe–Fe
Fe^{II}1	4+1	1	1.877(2)	1.907(2)	1.893	2.702	0.077	93.1(1)	87.0(1)	6.502
		3.7	1.879(3)	1.908(2)						
Fe^{II}1MeOH	5	1	1.879(2)	1.915(2)	1.902	2.329(2)	0.110	92.8(1)	86.8(1)	7.098
		3.3	1.906(2)	1.906(2)						
Fe^{II}2[e] Fe(1)	4	1	1.87	1.90	1.89	–	0.03	94	86	
		ca. 3.0	1.86	1.93						3.345
Fe(2)			1.93	1.95	1.91	–	0.04	93	87	4.503
			1.86	1.92						
$(Fe^{II}1)_2$dabco	5	1	1.886(2)	1.913(2)	1.900	2.338(2)	0.197	92.8(1)	86.1(1)	5.244[f]
		3.3	1.888(2)	1.914(2)						7.285[g]
$(Fe^{II}2)_2$dabco	5	1	1.895(2)	1.917(2)	1.906	2.326(2)	0.158	93.4(1)	85.8(1)	5.279[f]
		3.0	1.899(2)	1.912(2)						7.249[g]
$(Fe^{II}3)_2$dabco	5	1	1.894(5)	1.933(5)	1.913	2.327(5)	0.181	94.3	84.7(2)	4.211[f]
		3.1	1.896(5)	1.927(5)						7.274[g]
Fe^{III}1Cl	5	3/2	1.909(5)	1.920(5)	1.922	2.262(4)	0.405	90.2(2)	85.2(2)	6.217
		3.8	1.912(5)	1.948(5)						
Fe^{III}1I	5	3/2	1.892(3)	1.925(3)	1.906	2.637(1)	0.34	90.8(2)	85.4(2)	7.172
		4.2	1.884(3)	1.924(3)						
Fe^{III}1NO	5	1/2	1,928(2)	1.920(2)	1.924	1.732(2)	0.376			
		1.8	1.895(2)	1.954(2)						
$Fe^{II}Me_4$TAA	4	1	1.916	1.922	1.918	–	–0.114	95.5	84.1	5.909
			1.917	1.916						
$Fe^{II}(Me_4TAA)CO$	5		1.918	1.926	1.927	1.693	0.292	94.8	82.6	5.917
			1.933	1.931						
$Fe^{III}(Me_4TAA)Cl$	5	5/2	2.003	2.006	2.002	2.250	0.596	89.8	80.0	7.485
		6.0	1.995	2.005						

[a] Designation according to Figure 1. [b] Displacement of the iron atom from the main plane of the equatorial N-donor atoms. [c] Five-membered rings. [d] Six-membered rings. [e] The quality of the data is not sufficient and we are only publishing the conformation of the molecule, although distances and angles are similar to those of the other complexes. [f] Shortest distance between dinuclear units in the lattice. [g] Distance between dabco-bridged Fe atoms.

of the bridged complexes **(FeL)$_2$dabco** (**L** = **1**, **2**, **3**) were obtained. With imidazole and its derivatives the octahedral diadducts **FeL(HIm)$_2$** are strongly favoured. Sub-stoichiometric amounts of imidazole result in the formation of polymeric species.[17b,17c] In contrast, several iron(II) complexes of the general type **II** give mononuclear mono- and diadducts with imidazole.[5a] Additionally to the known pentacoordinate iron(III) complex **Fe^{III}1I** with axial iodide,[20] all the chlorides **Fe^{III}LCl** were isolated as solids, but only **Fe^{III}1Cl** gave crystals of sufficient quality. Selected parameters of the molecular structures and the magnetic moments at room temperature are listed in Table 1. The data of **Fe1I**,[20] **Fe1NO**,[22] **Fe(Me$_4$TAA)**,[16a] **Fe(Me$_4$TAA)CO**[16c] and **Fe(Me$_4$TAA)Cl**[16b] are included for comparison. The atom numbering in the table corresponds to that given in Figure 1. Figure 2 shows the molecular structures of selected examples, if possible approximately in the same projection of the basic chelate ring.

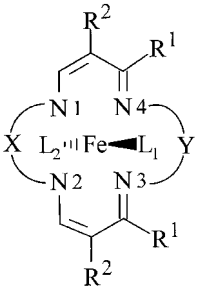

Figure 1. Unified atom numbering scheme used in Tables 1 and 3 for the equatorial donor atoms.

At first sight, the new data show few characteristic differences. The room-temperature magnetic moments are in satisfactory agreement with former measurements using a Gouy balance[17b] for **Fe1** (3.38 μ_B), **Fe1MeOH** (3.37 μ_B), **Fe1NH$_3$** (3.12 μ_B), **Fe1Py** (3.08 μ_B), and **Fe1I** (4.07 μ_B).[17c] These values are all higher to a greater or lesser degree than the spin-only value of 2.83 μ_B for two (S = 1) and 3.87 μ_B for three (S = 3/2) unpaired electrons, but all of them are within the region expected for intermediate-spin iron(II) and iron(III) complexes.[15a] (The reason for the increased values is probably a contribution of an orbital magnetic moment, due to an unsymmetrical population of the d_{xz} and d_{yz} orbitals, see also Figure 7.)

The iron atom has an approximately square-planar coordination sphere in **Fe2**. The central atom in all the other complexes is pentacoordinate with an approximately square-pyramidal geometry − in **Fe1** by intermolecular coordination of one of the peripheral carbonyl groups (*CN* = 4+1).The bond lengths and angles within the first coordina-

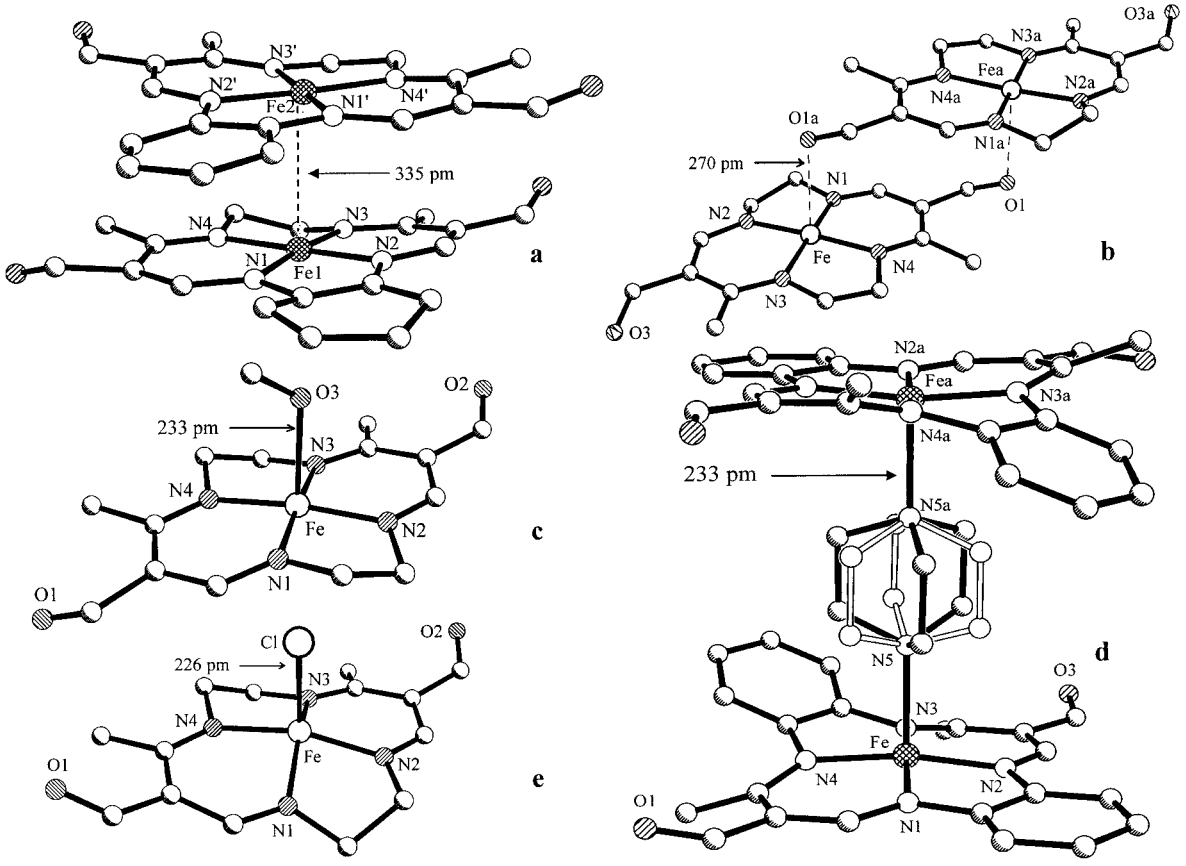

Figure 2. Molecule structures and coordination numbers *CN* of macrocyclic iron complexes: (a) **Fe^{II}2** (*CN* = 4), (b) **Fe^{II}1** (*CN* = 4+1), (c) **Fe^{II}1MeOH** (*CN* = 5), (d) **(Fe^{II}3)$_2$dabco** (*CN* = 5; the open lines represent the bonds of the 1:1 disorder), (e) **Fe^{III}1Cl** (*CN* = 5). Ethoxy groups are omitted for clarity.

tion sphere, including those of the octahedral complexes described in the next sections (cf. Table 3), reflect the rules formerly elaborated for a large number of our macrocyclic iron complexes:[5a] the Fe–N distances within the equatorial plane are, for low-spin and intermediate-spin complexes, nearly independent of the type of equatorial ligand $\mathbf{L^{2-}}$, the coordination number and the oxidation state of the central atom [average of 16 significant mean values from Tables 1 and 3 of 191(1) pm]. Larger differences exist between the Fe–N distances on the non-methylated side (N1, N2) and the methylated side (N3, N4) of the six-membered chelate rings [average of 32 significant values in each case: 189(1) and 192(1) pm, respectively]. The distances to the axial ligands are always longer than those within the equatorial plane. This is in contrast to the conditions in the case of many derivatives of (porphyrin)iron compounds and is obviously due to the higher effective field strength, which is accompanied by shorter equatorial Fe–N distances, of the ligands $\mathbf{L^{2-}}$ (**L** = **1**, **2**, **3**). The displacement of the central atom from the best equatorial [N_4] plane in pentacoordinate complexes is more obvious in the presence of relatively strong axial ligands with short distances to the iron atom (Cl^- > dabco > MeOH > COOEt) but there is no clear correlation. Interestingly, a small but significant displacement is also observed for the iron atom in $\mathbf{Fe^{II}2}$, which is directed towards the neighbouring iron atom in the asymmetric unit (Fe–Fe distance of 335 pm).

Two selected prototypes of complexes with a quite different behaviour are included in Table 1. The first one, the nitrosyl derivative **Fe1NO**, which we interpreted as $\mathbf{(Fe^{III})^{+}NO^{-}}$,[22a] has a temperature-independent $S = 1/2$ spin ground state. The axial Fe–N distance of 173 pm is shorter than the equatorial Fe–N bonds, which are approximately in the same range as for the other complexes. These deviations can be explained by assuming a very strong ligand field of the axial NO^- ligand. The other one, the pentacoordinate chloride complex **Fe(Me$_4$TAA)Cl**, which has a magnetic moment of 5.95 μ_B,[16b] is undoubtedly a high-spin iron(III) complex and resembles the behaviour of the pentacoordinate halides of (porphyrin)iron compounds. This is also reflected in an average Fe–N distance of over 200 pm that is typical for high-spin iron(II/III) complexes such as those of the general type **II**.[5a,22] Taking into account that the similar complex $\mathbf{Fe3^{III}Cl}$ is clearly an intermediate-spin complex (μ_{eff} = 4.20 μ_B at room temperature; structure data unfortunately not available), the difference indicates a lower field strength of the ligand **Me$_4$TAA**. The reason for this could be the stronger "saddle-shaped" distortion of the macrocycle, caused by the two additional methyl groups in R^3, and/or the absence of the peripheral carbonyl group in R^2, which increases the π-acceptor strength of the ligand and the effective charge of the central atom in the other complexes. In agreement with this idea, **Fe(Me$_4$TAA)** forms derivatives with carbon monoxide and other strong π-acceptors as axial ligand much more easily than **Fe3**.[16c,16d]

On closer inspection, the structural nuances of the complexes are reflected in the temperature dependence of the magnetic behaviour. Selected examples are depicted in Figure 3.

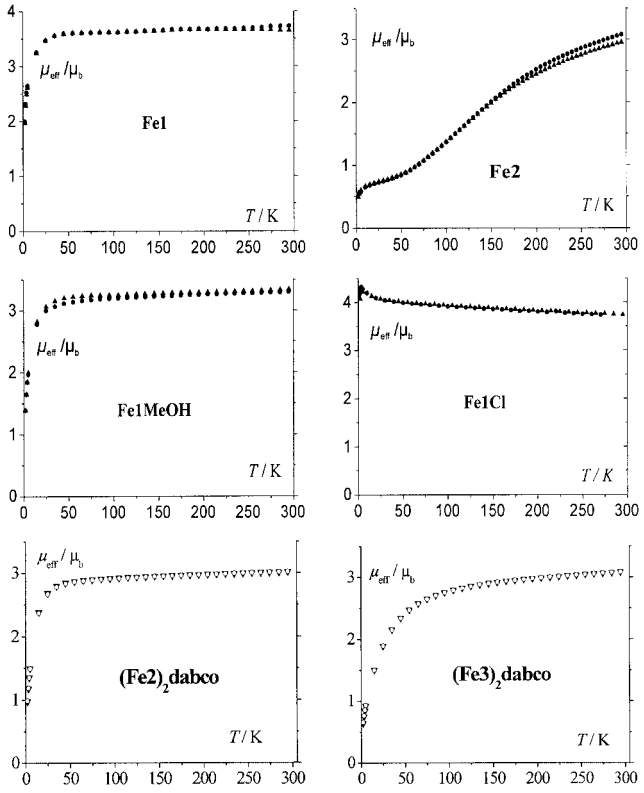

Figure 3. Temperature dependence of the effective magnetic moment of selected macrocyclic iron complexes: **Fe2** (*CN* = 4), **Fe1** (*CN* = 4+1), **Fe1MeOH**, **Fe1Cl**, **(Fe2)$_2$dabco**, **(Fe3)$_2$dabco** (all *CN* = 5). All measurements were carried out at 0.2 and 0.5 T.

With the exception of **Fe1Cl**, the magnetic moment decreases at lower temperature. **Fe2** shows a characteristic sigmoid curve progression which is apparent even at room temperature (Figure 3). This peculiarity can be explained as an incomplete and smooth transition into the low-spin $S = 0$ state, accompanied by antiferromagnetic interactions between two iron atoms (as mentioned above, the lattice of **Fe2** consists of pairs of two molecules with an iron–iron distance of 335 pm, which is short enough for direct interactions). The relatively steep decrease of the magnetic moment of several complexes at $T < 20$ K (left side of Figure 3) is not quite clear because the shortest Fe–Fe distance in the lattice is quite long (for **Fe1** and **Fe1MeOH** > 650 pm). In the case of the dinuclear iron(II) complex **(Fe3)$_2$dabco** the decrease of the magnetic moment starts already at $T < 150$ K. The Fe–Fe distances within the dinuclear unit are nearly identical for all **(FeL)$_2$dabco** derivatives (729, 725, and 727 pm for **L** = **1**, **2**, and **3**, respectively), but the Fe–Fe distances between the dinuclear units in the lattice are significantly shorter, especially for **(Fe3)$_2$dabco** (524, 528, and 421 pm for **L** = **1**, **2**, and **3**, respectively). This could explain the different behaviour of the latter.

The strong influence of the equatorial ligand is reflected in the zero-field Mössbauer spectra of solid samples of the

solvent-free complex **Fe1**. The spectrum at 4.2 K is given in Figure 4. The observed quadrupole splitting of ΔE_Q = 3.37 mm s^{-1} (isomer shift δ = 0.32 mm s^{-1}) is very large for an iron(II) complex, even if a square-planar coordination sphere is considered. The data for similar complexes are given in Table 2. ΔE_Q appears to increase with increasing σ-donating ability (basicity) of the equatorial ligand. This is in agreement with earlier observations revealing a stronger σ-donor ability of the ligands **1**–**3** in comparison to similar porphyrin ligands.

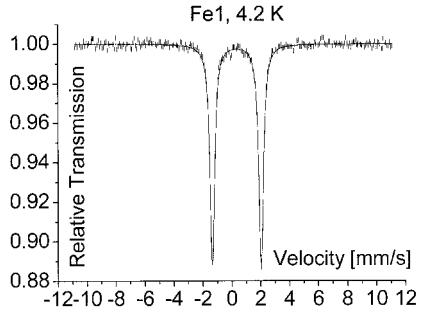

Figure 4. Mössbauer spectrum of **Fe^{II}1** at 4.2 K. Solid line: simulation of the spectrum with Lorentzian doublets.

Table 2. Mössbauer data of square-planar intermediate-spin (S = 1) iron(II) complexes.

Compound	Conditions	δ(Fe) [mm s^{-1}]	ΔE_Q [mm s^{-1}]	μ_{eff} [μ_B][a]	Ref.
Fe^{II}1	solid, 4.2 K	0.32	3.37	3.7	this work
Fe^{II}(TPP)	solid, 77 K	0.50	+1.51	4.4	[24a]
Fe^{II}(OEP)	solid, 83 K	0.59	+1.60	4.7	[24a]

[a] At room temperature.

The ESR spectrum of a frozen solution of **Fe1Cl** in toluene at 10 K is given in Figure 5. The g values (g_y^{eff} = 4.594, g_x^{eff} = 3.486 and g_z^{eff} = 2.039) can be assigned to the population of the ground-state (S = 1/2) Kramers doublet of the S = 3/2 system. The signal at 6.203 is due to small (μ-oxo?) impurities. The signal intensity of the impurity increases with decreasing temperature. The spectrum is similar to those reported for **Fe1I**,[20] although with slightly shifted g values, which can be assigned to a different rhombicity parameter E/D (D = axial, E = rhombic zero-field splitting parameter) of around 0.1 for the chloride complex (0.22 for the iodide adduct). In contrast to **Fe1I**, the chloride complex **Fe1Cl** is not ESR-silent in the solid state. A broad signal is observed at around g = 4.7, which can be explained by differences in the molecular packing in the crystal.

The intermediate-spin state of the iron(III) complexes is also reflected in the characteristic shifts of the resonances in the ^{1}H NMR spectra. As an example, the spectrum of

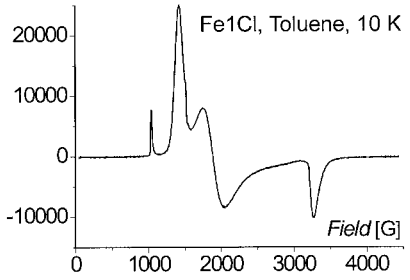

Figure 5. ESR spectrum of **Fe^{III}1Cl** in frozen toluene solution at 10 K.

Fe1Cl in toluene at 45 °C is given in Figure 6. With the help of predictions about the signal shifts based on literature proposals[25] and the signal intensities a clear assignment is possible. The observed paramagnetic shift can be interpreted by taking only the contact shift into account. The temperature dependence of the shifts obeys the Curie law.

Molecular orbital calculations based on the molecular structure were performed for **Fe1MeOH** and **Fe1Cl** to confirm the intermediate-spin ground state. Similar calculations were also performed for **Fe1I** and, for better comparison, the coordinate system was chosen the same way. The z axis of the molecular coordinate system was chosen in the direction of the axial ligand bond with the iron atom located at the origin of the coordinate system. The x and y axes are directed between the equatorial nitrogen atoms so that the σ-bonds with the equatorial ligand are formed by the $3d_{xy}$ orbital of the iron atom. The results of the spin-polarized calculations for **Fe1MeOH** are given in Figure 7.

The MO diagram of **Fe1Cl** is similar to that of **Fe1I** discussed in detail previously,[22] and is therefore not displayed here. Small differences are found in the bonding conditions between the iron atom and the axial ligand. In the case of the iodide adduct, covalent interactions between the $3d_{z^2}$ (σ-bonding) and $3d_{xz,yz}$ (weakly π-antibonding) orbitals of the iron atom and the $5p_z$ orbital of the axial ligand are present, while the $5p_{x,y}$ orbitals of the iodide ion are nearly non-bonding. In case of the chloride adduct π-interactions between the $3p_{x,y}$ orbitals of the chloride ion and the $3d_{xz,yz}$ orbitals of the iron atom are present and are more pronounced than in the case of the iodide adduct. This explains the hypsochromic shift of the typical LTMCT (equatorial *l*igand-*t*o-*m*etal *c*harge *t*ransfer) band in the UV/Vis spectrum of the chloride complex relative to the iodide one.[21]

The intermediate-spin state of **Fe1MeOH** is clearly mirrored in the molecular orbital diagrams. The unoccupied d_{xy} orbital responsible for the σ-bond with the equatorial ligand is clearly separated from the other four d orbitals and the strong interaction with the macrocycle leads to a reduced iron contribution. The interactions with the axial ligand (methanol) are not reflected in the MO diagrams, thereby indicating a very weak bond. The pattern of the MO energies is actually more similar to the typical pattern of a square-planar coordination than a square-pyramidal one, therefore the coordination number of the iron atom can also be described as 4+1.

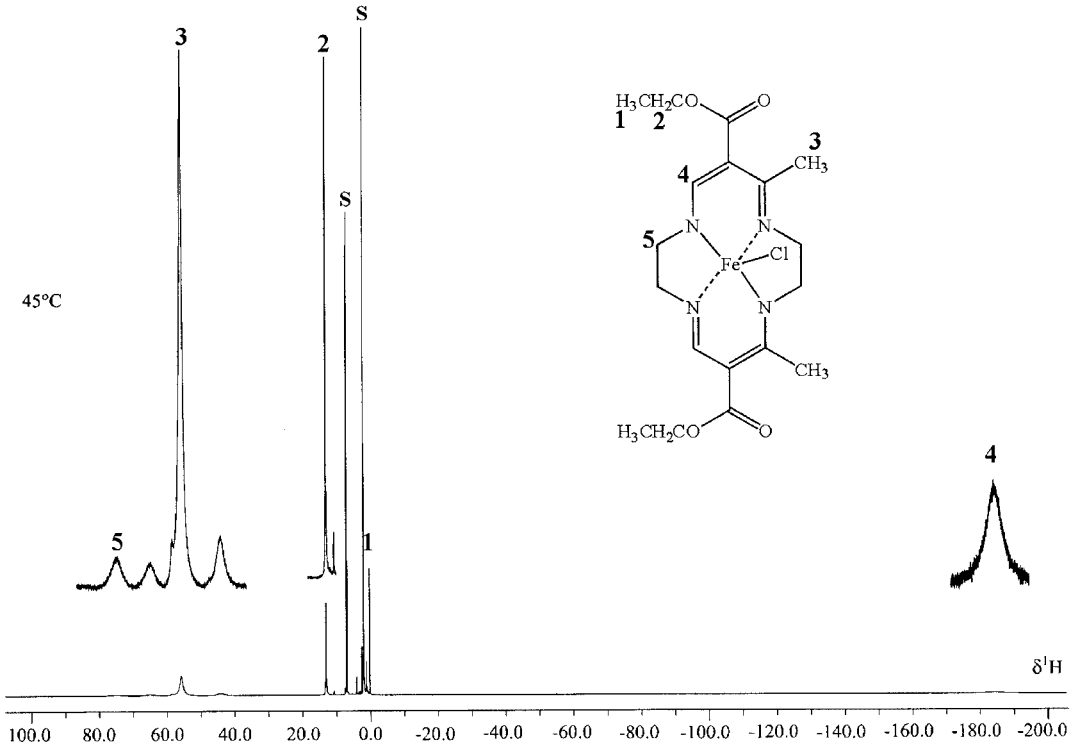

Figure 6. ^{1}H NMR spectrum and signal assignment of **Fe^{III}1Cl** in toluene solution at 45 °C. "S" denotes the solvent.

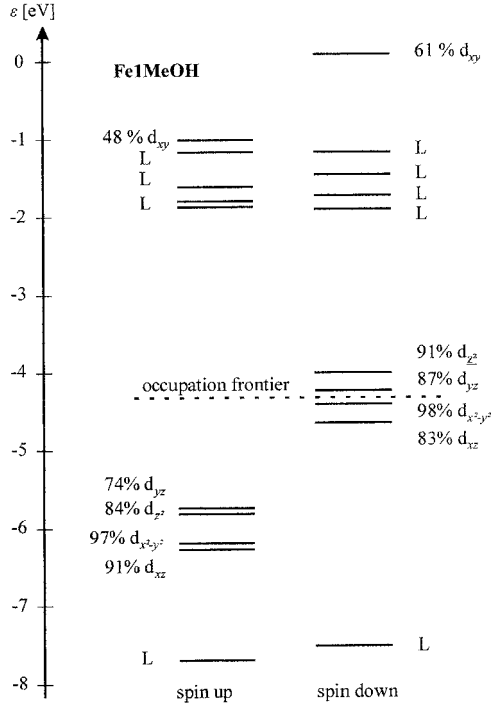

Figure 7. Orbital energies between 0 and –8 eV for the intermediate-spin state of **Fe1MeOH** for spin-polarised calculations. The approximate assignment for each level is given (L donates the equatorial ligand).

Orientation of Axial N-Heterocycles in Octahedral Complexes

One of the biological functions of b-type cytochromes is to switch the direction of charge-transfer processes depending on the potential. The active site contains haem with two axial imidazole rings of histidine. The voltage-dependent change of the orientation of the heterocyclic planes could be a possible mechanism for the switching. Former X-ray studies on the pair **Fe^{II}1(HIm)$_2$** and [**Fe^{III}1(HIm)$_2$**]-PF_6 gave evidence for such a charge-dependent reorientation of the imadazole planes,[18a] but it was not possible to clarify the role of the intermolecular hydrogen bonds in this case. Later on, an overview of the orientation of axial ligand planes in octahedral homo- and heteroligand diadducts of fifteen iron(II/III) complexes was given.[18b] We have now successfully crystallised **Fe^{II}3(Py)$_2$** and **[Fe^{III}3(Py)$_2$]**-PF_6, the first pair of complexes derived from the basic complex **Fe3**. The structures of both complexes are depicted in Figure 8 (right side), together with those of **Fe^{II}2Py$_2$** and [**Fe^{III}2Py$_2$**]ClO_4 (left side) for comparison. The corresponding bond lengths and angles are summarised in Table 3.

Addition of two neutral nitrogen ligands at the axial coordination sites of the macrocyclic iron complexes leads to low-spin complexes. The spin state was confirmed by ESR investigations in the case of the iron(III) complexes.[18b,19c] The iron atom is surrounded by six nitrogen atoms, resulting in a relatively symmetric close coordination sphere with an approximate D_{4h} symmetry. (Porphyrin)iron com-

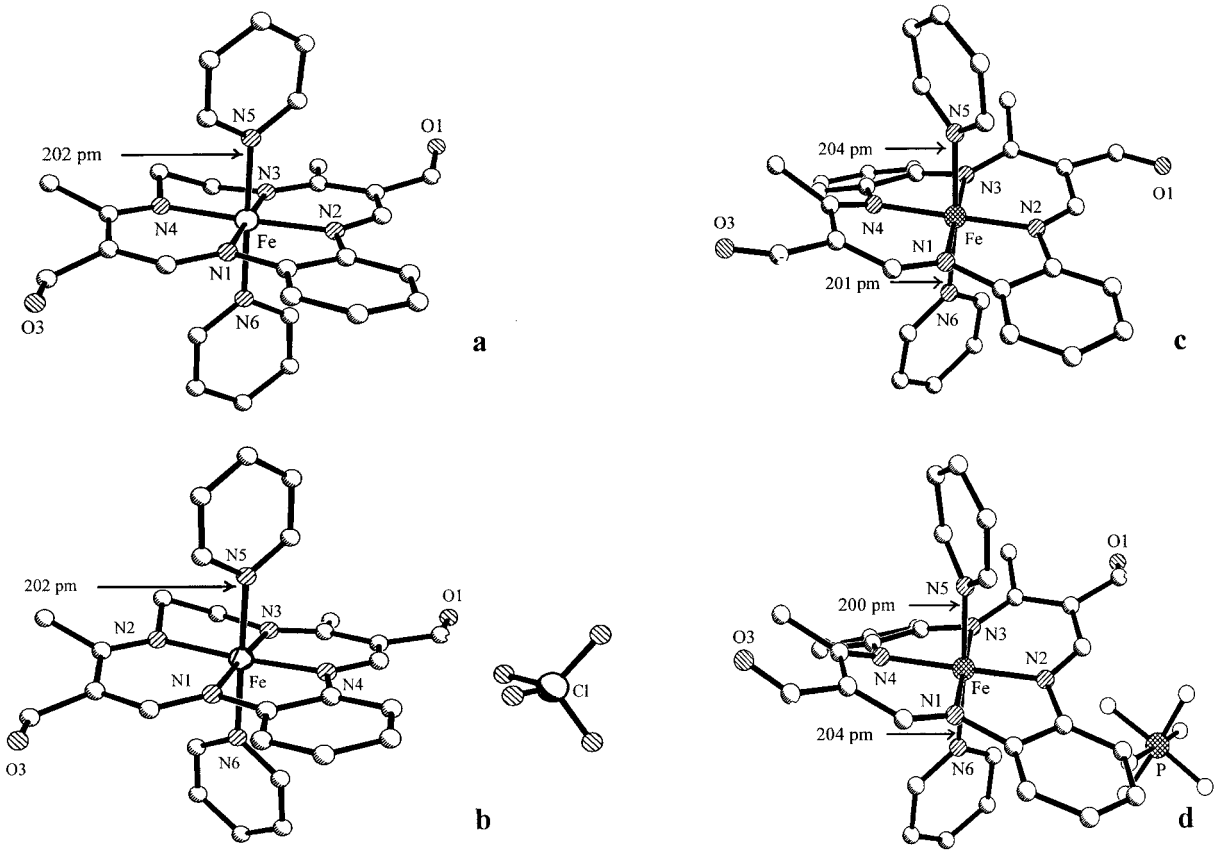

Figure 8. Molecule structures of (a) **$Fe^{II}2(Py)_2$**, (b) **[$Fe^{III}2(Py)_2$]ClO_4**, (c) **$Fe^{II}3(Py)_2$** and (d) **[$Fe^{III}3(Py)_2$]PF_6**. Ethoxy groups are omitted.

Table 3. Bond lengths [Å] and angles [°] within the first coordination sphere of macrocyclic iron(II/III) complexes with coordination number (*CN*) 6 and spin state *S*.

Complex	*CN*	S	Fe–$N_{1,2}$[a]	Fe–$N_{3,4}$[a]	Average FeL_{eq}	Fe–L_{ax}	Fe–pl_{eq}[b]	Angle $[L_{ax}]_{1\_2}$[c]
$[Fe^{III}1(Py)_2]PF_6$	6	1/2	1.882(5)	1.926(6)	1.899	2.045(3)	0.000	15
			1.893(6)	1.925(6)		2.063(3)		
$Fe^{II}2(Py)_2$[d]	6	0	1.917(2)	1.925(2)	1.920	2.018(2)	0.017	9
			1.904(2)	1.932(2)		2.037(2)		
$[Fe^{III}2(Py)_2]^+$[d]	6	1/2	1.893(2)	1.909(2)	1.902	2.022(2)	0.015	79
			1.887(2)	1.918(2)		2.040(2)		
$Fe^{II}3(Py)_2$	6	0	1.898(2)	1.934(2)	1.915	2.035(2)	0.010	90
			1.900(2)	1.929(2)		2.006(2)		
$[Fe^{III}3(Py)_2]^+$[e]	6	1/2	1.89	1.93	1.90	2.00	0.010	80
			1.90	1.90		2.04		
$[Fe^{III}1(N\text{-}MeIm)_2]^+$	6	1/2	1.893(6)	1.925(6)	1.907	2.017(7)	–	88
			1.882(5)	1.929(6)		2.001(6)		
$[Fe^{III}1(NCS)_2]^-$	6	1/2	1.896(2)	1.923(2)	1.909	1.947(3)	0.003	
			1.892(2)	1.926(2)		1.954(3)		
$[Fe^{III}2(CN)_2]^-$	6	1/2	1.910(2)	1.931(2)	1.918	2.002(3)	–	
			1.902(2)	1.930(2)		2.004(3)		
$[Fe^{III}2(NO_2)_2]^-$	6	1/2	1.887(3)	1.907(3)	1.901	1.982(3)	–	13
			1.895(2)	1.916(3)		2.000(3)		
$[Fe^{III}2(NO_2)OH_2]$	6	1/2	1.895(2)	1.925(3)	1.913	1.963(3)	0.018	
			1.904(3)	1.927(3)		2.055(4)		
$[Fe^{III}3(NO_2)NO]$ (?)[e,f]	6	0	1.85	1.90	1.89	2.00	0.032	
			1.91	1.91		1.96		

[a] Designation according to Figure 1. [b] Displacement of the iron atom from the main plane of the equatorial donor atoms. [c] Dihedral angle between the planes of the two axial ligands. [d] See ref.[18b] [e] The quality of the data is not sufficient and we are only publishing the conformation of the molecule, although distances and angles are similar to those of the other complexes. [f] Because of the disorder of the second axial NO_x ligand and the diamagnetism of the compound, the correct composition is uncertain.

pounds with similar axial ligands are also low-spin complexes, while complexes with sterically demanding axial ligands such as benzimidazole or 2-methylimidazole are high spin due to the small energetic splitting of the iron 3d orbitals.[26,27] Similar high-spin diadducts of our macrocycles have not been obtained up to now.

The iron atom is situated in the $[N_4]$ plane of the equatorial ligand. The average $Fe–N_{eq}$ bond lengths (190–192 pm) for both pairs in Figure 8 are in the range typical for all of our low-spin and intermediate-spin complexes, but significantly shorter than in similar (porphyrin)iron complexes (196–200 pm).[28] The change of the oxidation state of the iron atom from +2 to +3 leads to an almost negligible shortening of the equatorial bond lengths. A slight lengthening of these bonds in octahedral complexes of **Fe1** in comparison with the square-planar and pentacoordinate complexes can be explained by the increased electron density at the central atom. The bond lengths between the iron atom and the axial ligands are in the region 200–204 pm, similar to those in low-spin (porphyrin)iron complexes, and are independent of the oxidation state of the central atom.

The most characteristic difference between the structures of both pairs in Figure 8 is the orientation of the planes of the axial pyridine rings. In the case of **Fe^{II}2(Py)$_2$** both pyridine rings are nearly coplanar and are directed at the centre carbon atom of the six-membered chelate rings, similar to the case of **Fe^{II}1(Him)$_2$**. The angle between their planes amounts to only 9°. In the iron(III) derivative [**Fe^{III}2(Py)$_2$**]-ClO_4, however, both planes of the pyridine rings are twisted more in the direction at the equatorial N-atoms and the five-membered rings, and the angle between them is now 79°. This finding suggests that the similar behaviour of the pair **Fe^{II}1(Him)$_2$**/[**Fe^{III}1(Him)$_2$**]PF_6 is not necessarily a result of reorganisation of intermolecular hydrogen bonds. In contrast, the planes of the pyridine rings in the pair **Fe^{II}3(Py)$_2$** and [**Fe^{III}3(Py)$_2$**]PF_6 remain in a nearly unchanged orientation with an angle of 90° and 80°, respectively; they are independent of the oxidation state of the central atom. This is a consequence of the "saddle-shaped" distortion of the twofold phenylene-bridged equatorial ligand that allows only one energetically favoured orientation of the planes of the axial pyridine rings (perpendicular to each other) along the "trough" on each side.

All attempts to crystallise the iron(II) counterparts of [**Fe^{III}1(Py)$_2$**]PF_6 and [**Fe^{III}1(N-Meim)$_2$**]ClO_4 (Table 3) were unsuccessful.

Octahedral Complexes with Biologically Relevant Anions as Axial Ligands

Extended spectrophotometric equilibrium studies of the equilibria (1) and (2),[5a,5c,18b,19] particularly with the more hydrophilic complex **Fe1a**, have provided conclusive proof of the existence of octahedral iron(III) complexes [**Fe^{III}1aXY**] in solution with a large number of axial ligands, including anions as hydroxide, sulfite, nitrite, cyanide, thiocyanate, and even such "exotic" ligands as $[Fe(CN)_6]^{4-}$ and $[Fe(CN)_6]^{3-}$.[19a] In several cases, for example X = HIm, Y = CN^-, strong stabilizing interactions between both axial ligands have been detected.

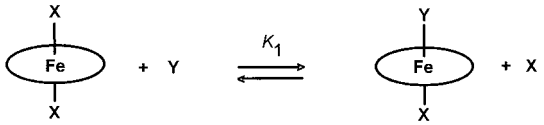

(1)

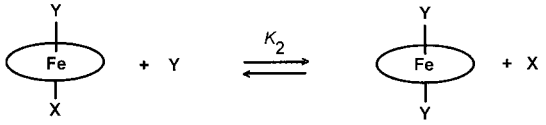

(2)

In view of the fact that anionic and mixed axial ligands play a key role in the chemistry of haem enzymes, we were interested in obtaining structural information for such complexes, especially to determine whether interactions between axial ligands through the central atom are reflected in the structural parameters. Unfortunately, attempts to isolate pure crystals failed in most cases, therefore only a few examples are presented here.

One of the many functions of haem enzymes in biological systems is the activation of small molecules and ions such as nitric oxide (NO), nitrite (NO_2^-) or sulfite (SO_3^{2-}). There has been a renewed interest in the biological nitrogen cycle with the discoveries of the biomedical functions of nitric oxide[29,30] and the clarification of the X-ray structure of the haem enzyme cytochrome c nitrite reductase.[31] This development increased the interest in model compounds with manageable electronic interactions to obtain a better understanding of the coherences of the biological activity of these small molecules. An overview of the properties of nitrosyliron complexes of ligand types **I** and **II** has been published.[22] A dinitrite adduct and several mononitrite adducts (with occupation of the sixth coordination site by other ligands) of "picket-fence" porphyrins have been prepared and several attempts have been made to describe the iron–nitrite bond.[32a–32d] All of these compounds are low-spin iron(III) complexes.

The reaction of our macrocyclic iron(II) complexes with nitrite under inert conditions yields the corresponding nitrosyliron complex as the main product, according to Equation (3), in all three cases. This was proved by ESR spectroscopy and by preparing **Fe1^{15}NO** using ^{15}N-labelled $NaNO_2$.

$$2\,\mathbf{Fe1} + 3\,NO_2^- + H_2O \rightarrow \mathbf{Fe1NO} + [\mathbf{Fe1(NO_2)_2}]^- + 2\,OH^- \quad (3)$$

The reaction of the iron(III) complexes with nitrite in organic solvents is even more complex. Although the spectrophotometric titration of [**Fe^{III}1a**]$^+$ clearly indicates the existence of a dinitrito and a mixed hydroxo-nitrito derivative in alkaline aqueous solution,[19b] all attempts to crystallise such derivatives of **Fe1** failed. Upon exclusion of air, the isolated reaction product of **Fe1Cl** or **Fe1I** in methanol is

the corresponding nitrosyl complex according to Equation (4). On the other hand, **Fe1NO** reacts in methanol or pyridine with air to give the nitrite adduct [Equation (5)]. The existence of a mono- and dinitrite adduct has been proved by UV/Vis spectroscopy.[22] Similar reactions have been found for ferric porphyrin complexes.[34]

$$\mathbf{Fe1}^{+} + 2\,NO_2^{-} \rightarrow \mathbf{Fe1NO} + NO_3^{-} \quad (4)$$

$$\mathbf{Fe1NO} + 1/2\,O_2 + D \rightarrow \mathbf{Fe1(NO_2)D};\ D = Py,\ MeOH \quad (5)$$

For **Fe2** it was possible, starting from the corresponding iodide or chloride complex, to isolate a nitrite diadduct and a few crystals of a mixed adduct with one nitrite ion and one water molecule as axial ligand *trans* to the nitrite ion. The molecule structures are given in Figure 9a, b. In both complexes the iron atom has a nearly octahedral coordination sphere and is located in the plane of the macrocycle. The Fe–N_{eq} and Fe–N_{NO_2} distances are similar to those of other diadducts. The oxygen atoms of the nitrite ligands point towards the six-membered chelate ring and, in the case of the diadduct, both nitrite groups are coplanar. The coordination of water in the case of the monoadduct is interesting. This has been postulated in many quantum-chemical investigations but has never been described in detail. The relatively large distance of 206 pm between the iron atom and the bound water molecule suggests a weak coordination.

While the nitrite diadduct is a pure low-spin complex over the whole temperature range, the nitrite monoadduct performs a spin transition between the S = 1/2 and S = 3/2 states. Such spin transition behaviour has already been reported for other six-coordinate iron(III) complexes[35a,35b] and is also typical of some nitrosyliron complexes of type **II**.[22,35c,35d] The effective moments plotted against temperature are given for both compounds in Figure 10.

Calculations based on the SCC-Xα method did confirm the S = 1/2 configuration as the ground state for both complexes. The energy difference to the S = 3/2 first excited state of **[Fe2(NO$_2$)OH$_2$]**(MeOH) is, at around 20 kJ mol^{-1}, small for this program. (The expected value at room temperature is significantly lower, but experience with the program used shows that the obtained values are within this region for this program.[40]) Therefore an admixture of this state and the ground state at room temperature is plausible. Another possibility is an interaction between both spin states that would explain the room-temperature effective moment of 2.82 μ_B, which is significantly lower than the expected spin-only value of 3.87 μ_B. Similar effects have been described in the literature for other iron(III) complexes.[36] Measurements of the effective magnetic moment at higher temperatures are not possible as the complex decomposes with loss of water. On the basis of these calculations it could be shown that the overlap population between Fe and O_{H_2O} decreases by 60% during the spin transition. The resulting pentacoordinate complex should be an intermediate-spin complex similar to the corresponding iron(III) halide complexes.

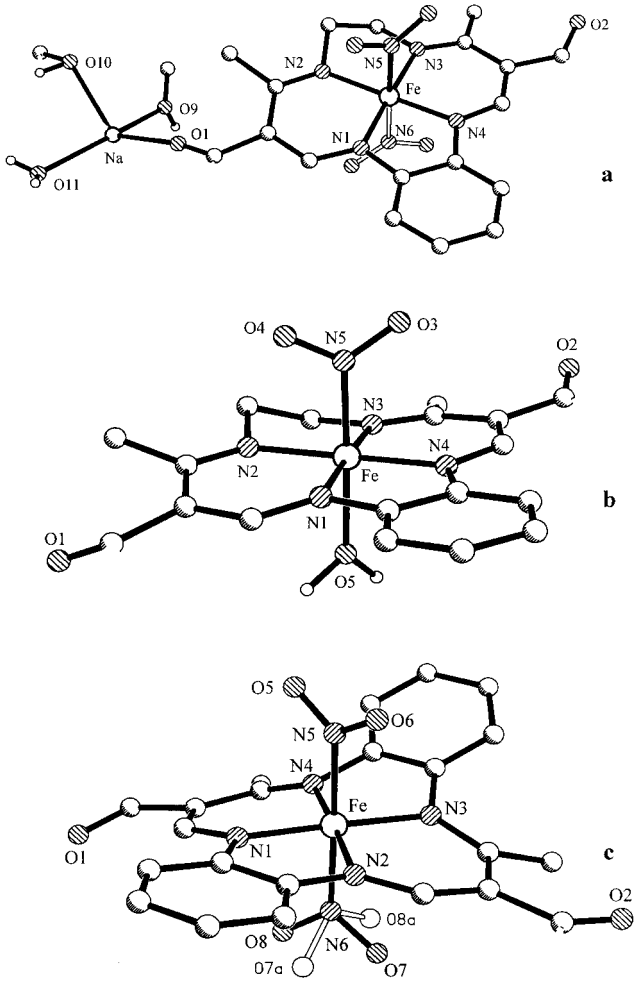

Figure 9. Molecule structures of (a) Na[**Fe^{III}2(NO$_2$)$_2$**](MeOH)$_2$(H$_2$O)$_{0.5}$, (b) [**Fe^{III}2(NO$_2$)OH$_2$**] and (c) [**Fe^{III}3(NO$_2$)NO$_x$**]$^-$. Ethoxy groups are omitted.

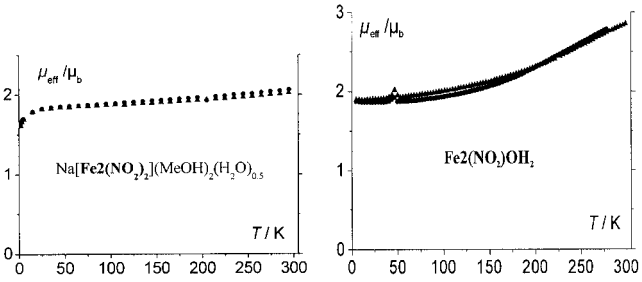

Figure 10. Temperature dependence of the effective magnetic moment of Na[**Fe^{III}2(NO$_2$)$_2$**](MeOH)$_2$(H$_2$O)$_{0.5}$ (left) and [**Fe^{III}2(NO$_2$)OH$_2$**] (right). The measurements were carried out at 0.2 and 0.5 T.

For **Fe3** − the complex most similar to (porphyrin)iron compounds − a derivative with the approximate composition (nBu$_4$N)$_2$[**Fe3(NO$_2$)NO$_x$**](NO$_2$)(H$_2$O), with one axial nitrite and one other axial NO_x ligand has been crystallised. Unfortunately, the latter is disordered in such a manner that it was impossible to decide between an NO_2 with two and an NO with four orientations. Additionally, the presence of

potential cations and anions in the lattice makes it more difficult to clearly define the charge of the central unit. The diamagnetism of the crystals suggests a neutral complex [**Fe^{III}3(NO$_2$)NO**] with low-spin iron(III), antiferromagnetically coupled with the nitrosyl radical. This interpretation agrees with the distances and angles within the central unit. Mixed axial nitrite-nitrosyl coordination has also been found in iron(II)[32e] and iron(III)[32d] complexes with "picket-fence" porphyrins.

The thiocyanate anion is of interest not only because of its biological relevance but also because it is, along with azide, one of the pseudo-halides that give heterogeneous equilibria with [**Fe^{III}1a**]$^+$ [Equation (6)] between aqueous and lipophilic phases accompanied by a "structural mimicry":

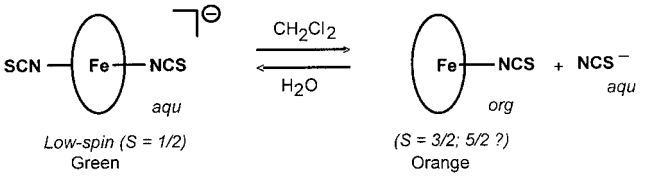

(6)

While the green product, in agreement with its EPR spectrum, is doubtless an octahedral low-spin iron(III) complex, the orange one, which is stable only in lipophilic solvents such as dichloromethane, benzene or toluene, has not been unambiguously characterised to date. Unfortunately, all attempts to obtain pure crystals of this product also failed. Crystals suitable for X-ray structure determination were only obtained for the diadduct [BzEt$_3$N][**Fe^{III}1(NCS)$_2$**].

The only examples of thiocyanato adducts of (porphyrin)-iron compounds described in the literature are a pentacoordinate monoadduct of high-spin iron(III)[37] and a hexacoordinate low-spin complex with pyridine as second axial ligand.[38] Cationic macrocyclic iron(II/III) complexes with neutral equatorial ligands easily form thiocyanato diadducts.[39] Thus, the complex [BzEt$_3$N][**Fe1(NCS)$_2$**] is the first macrocyclic iron complex with an anionic [N$_4$] ligand and two axially bound thiocyanate ligands (Figure 11).

For a proper description, the adduct has to be referred to as a diisothiocyanato complex, which is also the case for the corresponding porphyrin monoadducts. The linear coordination of the thiocyanate ion is confirmed by the Fe–N$_{ax}$–C$_{ax}$ angles of 171° and 179°. The Fe–N distances are comparable with those in cationic complexes described previously. The only conspicuous feature of the complex is the arrangement of the free ester groups of the equatorial ligand, where both carbonyl oxygen atoms point to the unsubstituted site of the ligand. For all other complexes of this ligand type characterised by X-ray structure analysis, at least one, but mostly both, of the terminal carbonyl oxygen atoms are directed towards the methyl group. The low-spin state of the iron(III) atom was confirmed by ESR spectroscopy (*g* values: 1.973, 2.125, 2.162).[18]

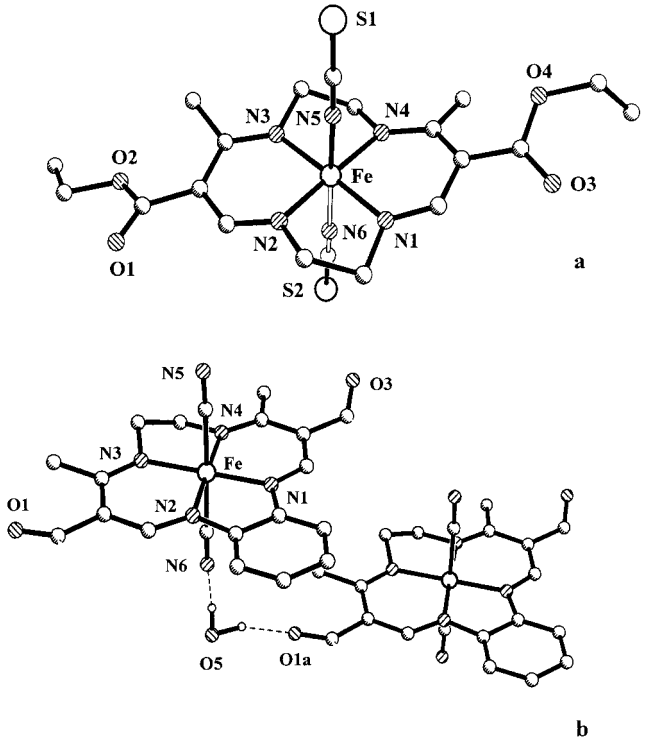

Figure 11. Molecule structures of (a) [**Fe^{III}1(NCS)$_2$**]$^-$ and (b) [**Fe^{III}2(CN)$_2$**]$^-$(H$_2$O)$_{0.5}$ (cations omitted for clarity).

An octahedral anionic complex with two cyanide ions as axial ligands, [Et$_4$N][**Fe^{III}2(CN)$_2$**] could be crystallised with the unsymmmetrically bridged macrocycle.

Dicyanide complexes are well documented and characterised in the literature.[41,42] The question as to whether the cyanide ion is bound to the iron atom through the carbon or the nitrogen atom was decided in favour of the carbon atom (the difference of the *R*1 values, the resulting C–N bond length and the remaining electron density were considered). This result fits with results in the literature. The distances between the iron atom and the equatorial nitrogen atoms are, with an average of 192 pm, slightly longer than those of other octahedral iron(III) complexes and are more comparable with those found for iron(II) complexes. Compared with the isothiocyanate diadduct, the axial bond lengths are also long and more similar to pyridine adducts. These differences in the bond lengths lead to the conclusion that in the case of cyanide as axial ligand, additional negative charge is localised at the iron atom (and therefore delocalised over the macrocyclic ligand), resulting in a lengthening of the bonds. In the case of the larger thiocyanate ion, the negative charge is localised on the easily polarizable sulfur rather than the iron atom, resulting in shorter bond. The low-spin state of the iron(III) atom was confirmed by ESR spectroscopy. In contrast to neutral octahedral complexes the ground-state electron configuration of the cyanide diadduct is $(d_{xz},d_{yz})^4(d_{xy})^1$. The same results can be found for comparable cyanide diadducts in the literature.[41,42]

Conclusions

The results described above confirm the close relation of our macrocycles with porphyrins, but they also indicate some special features. In general, the anions $\mathbf{L^{2-}}$ (**L** = **1**, **2**, **3**) seem to be stronger ligands for iron than most porphyrinato systems. The reasons for this could be: (i) the stronger basicity and σ-donor ability of the four nitrogen donor atoms, especially in the case of **L** = **1**; (ii) the presence of the electron-withdrawing carbonyl groups in conjugation with the π-system of the six-membered chelate rings, which promote potential π-backbonding and increase the effective charge of the central atom, especially when **L** = **2** and **3**, where the π-system is extended over one phenylene ring (the second phenylene in **3** is hardly included in the conjugation); (iii) the smaller hollow within the cavity of the 14-membered macrocycle, which is better suited for the radii of iron(II/III) in lower spin states.

The pronounced tendency to stabilize the intermediate-spin ground state in iron(II/III) complexes with coordination numbers below six, even when similar compounds are in a high-spin state [e.g. **Fe^{III}(Me$_4$TAA)Cl** or the halides of (porphyrin)iron compounds], is a typical feature of the ligands $\mathbf{L^{2-}}$. Intermediate spin (S = 1) was found in the iron(II) complexes **Fe2** (CN = 4, planar), **Fe1** (CN = 4+1 by weak intermolecular coordination of the ester carbonyl group), **Fe1MeOH** and the bridged complexes **(FeL)$_2$dabco** (**L** = **1**, **2**, **3**; all CN = 5, square-pyramidal). The preference to bind axial O-ligands − MeOH or even such a weak O-donor as COOEt − indicates that the iron atom in **Fe1** is the "hardest" central atom in the series **FeL**. The magnetic behaviour of the iron(II) complexes at lower temperature is often determined by intermolecular interactions in the lattice: **Fe2**, with the shortest Fe–Fe distance of 335 pm, shows a sigmoid decrease of the magnetic moment, whereas **(Fe3)$_2$dabco**, where the *inter*molecular Fe–Fe distance (421 pm) is much shorter than the *intra*molecular distance (727 pm), shows a steep decrease of the moment starting already at around 150 K. The complexes **FeLCl** (**L** = **1**, **2**, **3**) and the iodide **Fe1I** represent the iron(III) case of intermediate-spin (S = 3/2) behaviour. The intermediate-spin state could be confirmed by Mössbauer spectrometry for **Fe1**, by ESR and NMR spectroscopy for **Fe1Cl**, and by DFT-MO calculations for **Fe1MeOH**, **Fe1Cl** and, previously, for **Fe1I** (see refs.[22b,22c] for more calculations).

The pair **Fe^{II}3(Py)$_2$**/[**Fe^{III}3(Py)$_2$**]PF_6 was characterised as a third example of potential "voltage-dependent molecular switches" based on octahedral low-spin iron(II/III) complexes with N-heterocycles as axial ligands. Comparison with the pairs **Fe^{II}1(HIm)$_2$**/[**Fe^{III}1(HIm)$_2$**]PF_6 and **Fe^{II}2(Py)$_2$**/[**Fe^{III}2(Py$_2$)**]ClO_4 resulted in the conclusions that: (i) the charge-dependent change of the orientation of the axial planes is not necessarily accompanied by reorganisation of intermolecular hydrogen bonds, and (ii) the "saddle-shaped" distortion of the ligand **3** allows only orientation of the axial planes perpendicular to each other; no charge-dependent twist of these planes is possible. Other new octahedral low-spin complexes with axial N-heterocycles are [**Fe^{III}1(Py)$_2$**]PF_6 and [**Fe^{III}1(N-MeIm)$_2$**]ClO_4, but unfortunately their iron(II) counterparts could not be obtained as suitable crystals.

Octahedral low-spin derivatives of the macrocyclic iron complexes **FeL** with biologically relevant anions as axial ligands have been crystallised for the first time, although their existence in solution was proved many years ago. Reactions with nitrite resulted in the anionic diadduct [**Fe^{III}2(NO$_2$)$_2$**]$^-$ with pentacoordinate sodium as counterion, and, more interestingly, in the neutral mixed-ligand complex [**Fe^{III}2(NO$_2$)OH$_2$**]. The presence of water as a relatively weak axial ligand results in a temperature-dependent admixing of low-spin (favoured at low temperature) and, possibly, intermediate-spin species. DFT-MO calculations agree with this interpretation. With cyanide and thiocyanate ions the octahedral low-spin diadducts [Et_4N][**Fe2(CN)$_2$**] and [$BzEt_3N$][**Fe1(NCS)$_2$**] could be crystallised. Unfortunately, it was not possible to obtain pure crystals of the pentacoordinate neutral counterpart of the latter, **Fe^{III}1(NCS)**, which exists together with the anionic diadduct in an equilibrium of distribution between a lipophilic and an aqueous phase.

With regard to the existence of high-spin iron(II/III) complexes and to the processes of spin conversion, some of the iron complexes of type **II** are more closely related to (porphyrin)iron compounds than the macrocycles **I**. This will be the subject of a following paper.

Experimental Section

General Procedures and Instrumentation: If not stated differently, all syntheses were carried out under argon using Schlenk tube techniques. All solvents were purified as described in the literature[43] and distilled under argon. Magnetic measurements of pulverized samples were performed with a Quantum Design MPMSR-5s SQUID magnetometer in a temperature range from 1.7 to 400 K, with the exception of **Fe2Cl** and **Fe3Cl**. All measurements were carried out at two field strengths (0.2 and 0.5 T). Diamagnetic corrections were made using values calculated with tabulated Pascal constants (as a rule, suitable values can be estimated as $\chi_{dia} \approx 0.6 \times 10^{-6} M_{complex}$). The measurements of the highly air-sensitive iron(II) compounds were repeated several times under strongly inert conditions to ensure that the samples remain in the iron(II) state during preparation. For comparison, an additional sample was measured after exposure to air. ESR investigations were carried out with an ESP 300E (Bruker) instrument at liquid-nitrogen temperature with the solid or in solution (methanol, toluene) or equipped with an N_2/He-flow cryostat from 4.2 K up to room temperature. Molecular orbital calculations were carried out in a local density approximation (LDA) by the spin-polarized self-consistent-charge (SCC-)Xα method.[44,45]

Syntheses: The syntheses of the free ligands are summarised in Scheme 2 for **H$_2$1** and **H$_2$2** and in Scheme 3 for **H$_2$3**. All steps of the ligand syntheses were carried out in air. From a thermodynamic point of view, the driving force of the complex formation starting from the free ligand, as well as of the reverse protolysis of the complex, depends on the competition between two protons and the divalent metal ion to bind the anion of the deprotonated ligand:

$$M^{2+} + 2HL \rightleftharpoons ML + 2H^+ \quad (7)$$

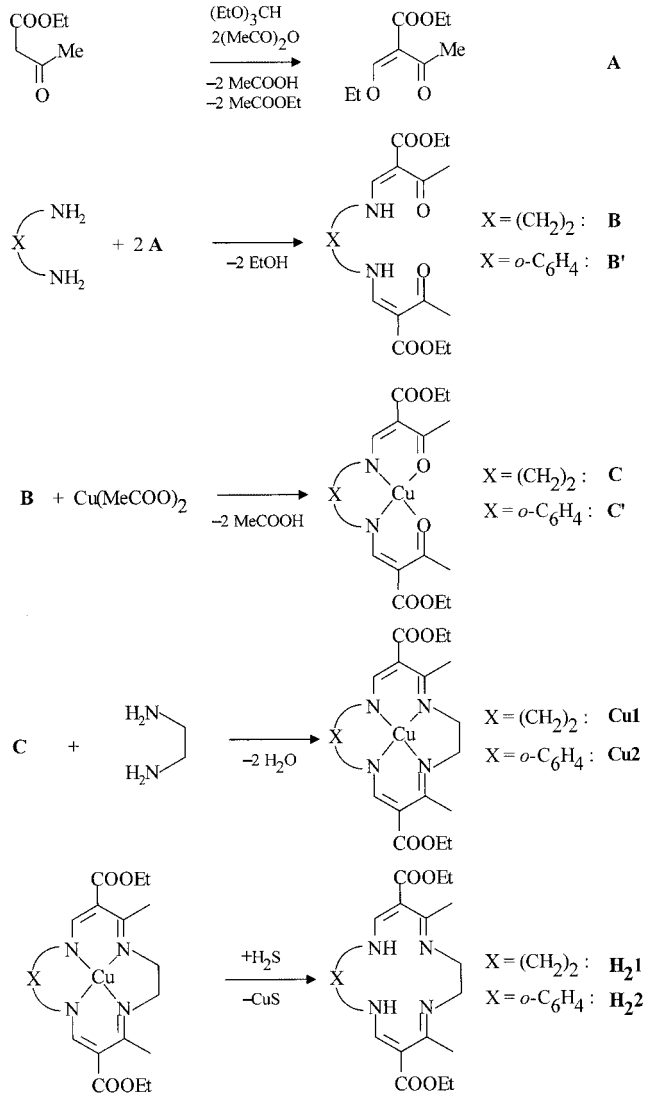

Scheme 2. Syntheses of the free macrocyclic ligands H_2**1** and H_2**2**.

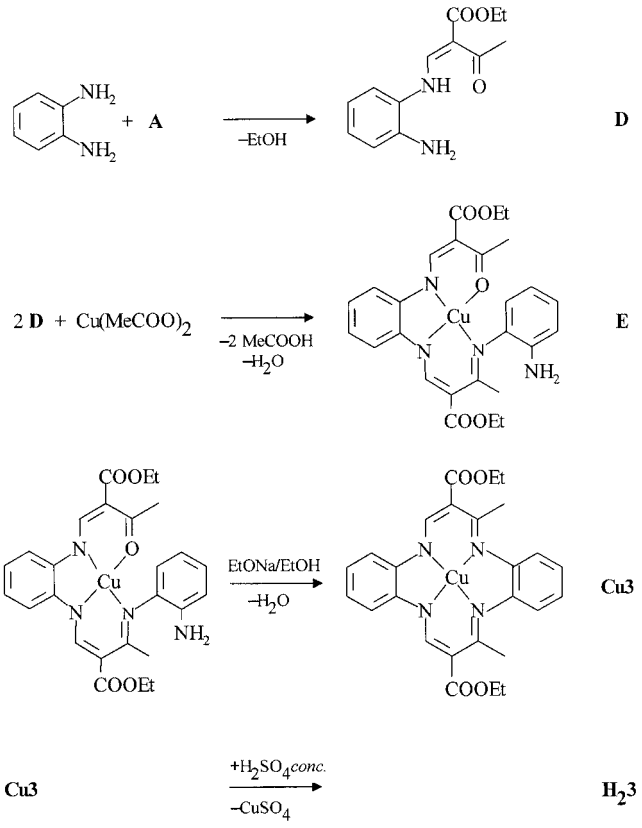

Scheme 3. Synthesis of the free macrocyclic ligand H_2**3**. The Cu-driven condensation of two molecules **D** is expected to give the *anti* isomer of the copper complex **E** with respect to the methyl groups. The X-ray analysis of **E** confirms, however, the depicted *syn* structure.[14b]

The key step of the syntheses of the free ligands is a template reaction using the copper(II) ion as template, followed by the demetallation of the macrocyclic copper complex. The different conditions of the demetallation reflect the different properties of the ligands: the release of the protonated macrocycle H_2**3** from **Cu3** is possible by dissolving it in sulfuric acid without any auxiliary reagent. This is obviously due to the relatively low stability of the copper complex **Cu3**, where the copper(II) ion is too large for the small hollow of the rigid anion $\mathbf{3}^{2-}$. To obtain the ligands H_2**1** and H_2**2**, addition of the auxiliary reagent hydrogen sulfide is necessary to remove the copper ion. Different reaction conditions are also typical for the formation of iron complexes. As in the case of porphyrins, iron(II) is easier to incorporate into the macrocycles than iron(III). The complex **Fe1** was formed nearly quantitatively in a fast reaction using a 1:1 ratio of ligand and iron(II) acetate, even under moderate basic conditions. For the complexes **Fe2** and **Fe3** an excess of the iron(II) salt is necessary to prevent contamination by the free ligand. Additionally, the complex formation requires an increase of the reaction time from a few minutes (**Fe1**) to 2–3 h (**Fe2**) or 10–11 h (**Fe3**). This increase reflects the kinetic effect of the increasing rigidity of the ligand structures.

Syntheses of the Macrocyclic Ligands

6,13-Bis(ethoxycarbonyl)-7,12-dimethyl-1,4,8,11-tetraazacyclotetradeca-5,7,12,14-tetraene ($H_2$1):[17b,46b] The preparation of this ligand by a template synthesis of the copper complex **Cu1**, followed by demetallation with hydrogen sulfide in dilute sulfuric acid and precipitation with sodium hydroxide, gave the free ligand in nearly quantitative yield. However, to prevent the use of gaseous hydrogen sulfide, the latter can be replaced by precipitation from homogeneous solution by in situ hydrolysis with thioacetamide. In this case the yield of the last step drops to about 45%.

Compound A:[47] Ethyl acetoacetate (130 g, 1 mol), acetic anhydride (204 g, 2 mol) and triethyl orthoformate (148 g, 1 mol) were refluxed together for 40 min. The low-boiling side-products were distilled off at normal pressure until foggy clouds appeared in the reaction vessel. The main product was then obtained by fractionatal vacuum distillation (b.p. 145–150 °C at 2 kPa). The purity of the oily, colourless to bright greenish-yellow product was determined by GC analysis. Yield: 140.1 g (75%).

Compound B:[33] Compound **A** (140.1 g, 0.75 mol) was dissolved in methanol (130 mL) and freshly distilled ethylenediamine (22.8 g, 0.379 mol), dissolved in methanol (130 mL), was then slowly added to the solution. The reaction mixture was stirred vigorously and the ligand precipitated immediately. The colourless product was filtered off and recrystallised from ethanol or dioxane. Yield: 94 g (77%).

Compound C:[33] Compound **B** (10 g, 0.029 mol) and copper acetate monohydrate (5.9 g, 0.035 mol, finely pulverized) were mixed and

heated in DMF or ethanol (500 mL) to reflux for 30 min. After cooling, violet crystals precipitated that were filtered off, washed with methanol and dried. Yield: 10.1 g (85%).

Cu1:[46a] Compound **C** (50 g, 0.12 mol) was dissolved in ethylenediamine (100 mL, dried and freshly distilled from solid potassium hydroxide) and heated to reflux until the colour had changed from deep blue to brownish-violet (15–30 min). After cooling, the product was filtered off and washed with water. Yield: 38.5 g (72%).

$H_2$1:[17b,46b] **Cu1** (2.0 g, 0.0047 mol) was suspended in methanol (10 mL) and stirred for 15 min. Ice-cold (0 °C) dilute sulfuric acid (ca. 2 M, 40 mL) was then added to the suspension. After 1 min, thioacetamide (4.2 g, 0.056 mol) was added to the suspension and the reaction mixture was stirred for a further 3 min. The suspension was filtered through a fluted filter paper into a calculated volume of ice-cold sodium hydroxide solution (ca. 4 M) such that the mixture became neutral or weakly basic after addition of all of the acidic filtrate. The free ligand was filtered off and washed with water until a nearly neutral pH was obtained. The crude material was recrystallised from methanol as fine colourless needles. Yield: 0.8–1 g (47–58%).

6,13-Bis(ethoxycarbonyl)-7,12-dimethylbenzo[*b*]-1,4,8,11-tetraazacyclotetradeca-5,7,12,14-tetraene ($H_2$2): Cu2 was synthesised in analogy to **Cu1** using 1,2-phenylenediamine instead of ethylenediamine in step **B**.[10d,33]

$H_2$2:[10d] **Cu2** (2.0 g, 0.0042 mol) was suspended in methanol (10 mL) and stirred for 15 min. Ice-cold (0 °C) sulfuric acid (5 M, 40 mL) was then added to the suspension. After 1 min, thioacetamide (4.2 g, 0.056 mol) was added to the suspension and the reaction mixture was stirred for a further 3 min. The suspension was then filtered into ice-cold sodium hydroxide (4 M, 100 mL) taking care to ensure that the solution did not warm up. The free ligand was filtered off and washed with water until a nearly neutral pH was obtained. The crude material was dissolved in a little dioxane and reprecipitated with distilled water to obtain yellow crystals. Yield: 0.8–1 g (45–60%).

6,13-Bis(ethoxycarbonyl)-7,12-dimethyldibenzo[*b*,*i*]-1,4,8,11-tetraazacyclotetradeca-5,7,12,14-tetraene ($H_2$3):[23a] In earlier reports, the complexes **M3** (M = Cu, Co)[23c] and the intermediates **E**[23b] were postulated as isomeric structures with an *anti* configuration of the methyl groups attached to the six-membered chelate rings. However, the X-ray structural analysis of the free ligand **$H_2$3** and the nitrosylcobalt complex **Co3NO** proved the *syn* structure.[14b]

Compound D:[23b] A suspension of *o*-phenylenediamine (12 g, 0.11 mol) in ethanol (100 mL) was heated to reflux. Compound **A** (18.6 g, 0.1 mol) was slowly added to the solution and the mixture was refluxed for 20 min. After cooling, compound **D** precipitated as yellow needles that were collected and recrystallised twice from methanol or ethanol. Yield: 13.14 g (53%). M.p. 84 °C.

Compound E:[23b] Compound **D** (24.8 g, 0.1 mol) was heated to reflux in methanol (200 mL) and a suspension of finely ground copper acetate monohydrate (9.98 g, 0.05 mol) in methanol (150 mL) was slowly added to the solution. The suspension was refluxed for approximately 6 h. After cooling, the product was filtered off immediately, washed with methanol and dried. Yield: 23.56 g (87%).

Cu3:[23c] Compound **E** (6.68 g, 0.012 mol) was heated to reflux in dry ethanol (150 mL). Metallic sodium (0.31 g, 0.013 mol), dissolved in dry ethanol (50 mL), was slowly added to the suspension and the mixture refluxed for 6 h. After cooling, the product was filtered off immediately, washed with cold methanol and dried. Yield: 5.99 g (96%).

$H_2$3:[23a] **Cu3** (2 g, 0.0038 mol) was suspended in cooled concentrated H_2SO_4 (50 mL) where it underwent a colour change from brown to yellow. The suspension was added dropwise to a water/ice mixture, taking care to ensure the solution did not warm up. The free ligand precipitated as yellow needles that were collected on a paper filter, washed with water until a neutral pH was obtained, and dried at room temperature. The crude material was dissolved in a little dioxane and reprecipitated with distilled water to obtain yellow crystals. Yield: 1.2–1.4 g (70–80%).

Syntheses of the Iron(II) Complexes

[6,13-Bis(ethoxycarbonyl)-7,12-dimethyl-1,4,8,11-tetraazacyclotetradeca-5,7,12,14-tetraenato(2–)]iron(II) (Fe1):[17b] Iron(II) acetate (2.08 g, 11.9 mmol) and **$H_2$1** (4.30 g, 11.8 mmol) were dissolved in methanol (60 mL) and refluxed for 1 h. After standing overnight, the red precipitate was collected and dried in vacuo. Yield: 2.27 g (46%). $C_{18}H_{26}FeN_4O_4$ (418.27): calcd. C 51.68, H 6.27, N 13.40; found C 48.34, H 6.09, N 12.22; the discrepancy between the calcd. and found values is due to the high air sensitivity of the complex. IR (Nujol): $\nu_{C=O}$ = 1671 cm^{-1}. MS (DEI): *m*/*z* (%) = 418 (100) [M^+], 373 (15) [$M^+ - OC_2H_5$], 344 (5) [M^+ – COOEt].

[6,13-Bis(ethoxycarbonyl)-7,12-dimethylbenzo[*b*]-1,4,8,11-tetraazacyclotetradeca-5,7,12,14-tetraenato(2–)]iron(II) (Fe2):[10d] Iron(II) acetate (0.76 g, 4.4 mmol) and **$H_2$2** (1.27 g, 3.1 mmol) were suspended in methanol (20 mL) and refluxed for 6 h. The black product was collected, washed with a small volume of methanol and dried in vacuo. Yield: 1.14 g (77%). $C_{22}H_{26}FeN_4O_4$ (466.31): calcd. C 56.66, H 5.62, Fe 11.98, N 12.02; found C 55.23, H 5.52, Fe 12.1, N 12.24; the discrepancy between the calcd. and found values is due to the high air sensitivity of the complex. IR (Nujol): $\nu_{C=O}$ = 1676 cm^{-1}. MS (DEI): *m*/*z* (%) = 43 (100), 466 (50) [M^+].

[6,13-Bis(ethoxycarbonyl)-7,12-dimethyldibenzo[*b*,*i*]-1,4,8,11-tetraazacyclotetradeca-5,7,12,14-tetraenato(2–)]iron(II) (Fe3):[23a] Iron(II) acetate (1.33 g, 7.7 mmol) and **$H_2$3** (2.29 g, 5.0 mmol) were suspended in methanol (20 mL) and refluxed for 12 h. The black product was collected, washed with a small volume of methanol and dried in vacuo. Yield: 2.24 g (88%). $C_{26}H_{26}FeN_4O_4$ (514.35): calcd. C 60.71, H 5.09, N 10.89; found C 59.95, H 5.09, N 11.01. IR (Nujol): $\nu_{C=O}$ = 1686 cm^{-1}. MS (DEI): *m*/*z* (%) = 514 (100) [M^+], 486 (20) [$M^+ - C_2H_4$], 468 (15) [$M^+ - OC_2H_5$].

Dinuclear Adducts with Bridging 1,4-Diazabicyclo[2.2.2]octane (dabco)

(Fe1)$_2$dabco: Iron(II) acetate (0.31 g, 1.8 mmol) and 0.65 g of **$H_2$1** were dissolved in 20 mL of methanol and refluxed for 20 min. After cooling, a solution of dabco (0.2 g, 1.8 mmol) in 5 mL of methanol was slowly added to the solution. Slow crystallisation overnight yielded red needles suitable for X-ray structure analysis. The product was collected, washed with a little ice-cold methanol and dried in vacuo. Yield: 0.33 g (39%). $C_{36}H_{52}Fe_2N_8O_8 \cdot C_6H_{12}N_2$ (948.73): calcd. C 53.71, H 6.80, N 14.77; found C 52.48, H 6.59, N 14.78. IR (Nujol): $\nu_{C=O}$ = 1673, 1652 cm^{-1}. MS (DEI): *m*/*z* (%) = 112 (100) [M^+(dabco)], 418 (90) [M^+(**Fe1**)]. DTG: Up to 250 °C loss of 11.3% (calcd. for 1 dabco: 11.8%); decomposition at 300 °C.

(Fe2)$_2$dabco: Fe2 (0.5 g, 1.1 mmol) was suspended in 20 mL of methanol. Then, 1.3 mL of a 1 M solution of dabco in methanol was added to the suspension and left standing for slow crystallisation. After 2 d, red-black needles were obtained. The product was collected, washed with a little methanol and dried in vacuo. Yield: 0.3 g (55%). $C_{44}H_{52}Fe_2N_8O_8 \cdot C_6H_{12}N_2$ (1044.8): calcd. C 57.48, H 6.18, N 13.42; found C 56.60, H 6.12, N 13.41. IR (Nujol): $\nu_{C=O}$ = 1674 cm^{-1}. MS (DEI): *m*/*z* (%) = 112 (100) [M^+(dabco)], 466 (10) [M^+(**Fe2**)]. DTG: Up to 100 °C loss of 11.3% (solvent in the crys-

tal), up to 300 °C loss of 12.4% (calcd. for 1 dabco: 10.7%); decomposition at 350 °C.

$(Fe3)_2$dabco: Fe3 (0.65 g, 1.3 mmol) was suspended in 40 mL of methanol. Then, 1.8 mL of a 1 M solution of dabco in methanol was added to the suspension and left standing for slow crystallisation. After 2 d, black needles were obtained. The product was collected, washed with a little methanol and dried in vacuo. Yield: 0.45 g (61%). $C_{52}H_{52}Fe_2N_8O_8 \cdot C_6H_{12}N_2$ (1140.9): calcd. C 61.06, H 5.65, N 12.28; found C 58.96, H 5.90, N 12.03. IR (Nujol): $\nu_{C=O}$ = 1686 cm^{-1}. MS (DEI): *m*/*z* (%) = 42 [fragment], 112 (90) [M^+(dabco)], 514 (10) [M^+(**Fe3**)]. DTG: Up to 250 °C loss of 9.7% (calcd. for 1 dabco: 9.8%); at 350 °C decomposition.

Syntheses of the Iron(III) Complexes: The syntheses of the iron(III) iodide complexes **Fe1I**[19c,21] and **Fe2I**[10d] have been described previously.

[6,13-Bis(ethoxycarbonyl)-7,12-dimethyl-1,4,8,11-tetraazacyclotetradeca-5,7,12,14-tetraenato(2–)]iron(III) Chloride (Fe1Cl): Fe1 (1.36 g, 3.3 mmol) was suspended in tetrachloromethane (20 mL) for 2 d. The CCl_4 was then removed by cold vacuum distillation and the obtained solid was recrystallised from methanol. The precipitate was filtered off and dried in vacuo. The mother solution was allowed to stand overnight to produce single crystals of **Fe1Cl** suitable for X-ray crystallography. Yield: 1.04 g (69%). $C_{18}H_{26}ClFeN_4O_4$ (453.72): calcd. C 47.65, H 5.78, N 12.35; found C 44.81, H 5.37, N 11.50. IR (Nujol): $\nu_{C=O}$ = 1680 cm^{-1}. MS (DEI): *m*/*z* (%) = 28 (100), 453 (10) [M^+], 418 (30) [M^+ – Cl]. DTG: Decomposition at 170 °C.

[6,13-Bis(ethoxycarbonyl)-7,12-dimethylbenzo[*b*]-1,4,8,11-tetraazacyclotetradeca-5,7,12,14-tetraenato(2–)]iron(III) Chloride (Fe2Cl): Fe2 (0.67 g, 1.4 mmol) was suspended in tetrachloromethane (20 mL) for 2 d. The CCl_4 was then removed by cold vacuum distillation and the solid product was recrystallised from methanol. The precipitate was filtered off and dried in vacuo. Yield: 0.59 g (84%). $C_{22}H_{26}ClFeN_4O_4$ (501.764): calcd. C 52.66, H 5.22, N 11.17; found C 52.52, H 4.89, N 11.45. IR (Nujol): $\nu_{C=O}$ = 1685 cm^{-1}. MS (DEI): *m*/*z* (%) = 36 (100), 501 (50) [M^+], 466 (20) [M^+ – Cl].

[6,13-Bis(ethoxycarbonyl)-7,12-dimethyldibenzo[*b*,*i*]-1,4,8,11-tetraazacyclotetradeca-5,7,12,14-tetraenato(2–)]iron(III) Chloride (Fe3Cl): Fe3 (0.96 g, 1.9 mmol) was suspended in tetrachloromethane (30 mL) for 2 d. The CCl_4 was then removed by cold vacuum distillation and the solid was recrystallised from methanol. The precipitate was filtered off and dried in vacuo. Yield: 0.87 g (83%). $C_{26}H_{26}ClFeN_4O_4$ (549.80): calcd. C 56.79, H 4.77, N 10.19; found C 55.60, H 4.61, N 10.48. IR (Nujol): $\nu_{C=O}$ = 1697 cm^{-1}. MS (DEI): *m*/*z* (%) = 31 (100), 549 (90) [M^+], 514 (15) [M^+ – Cl].

Synthesis of Diadducts of Iron(II/III) Complexes

$Fe3(Py)_2$: Fe3 (40 mg) was dissolved in pyridine (7 mL) and a layer of heptane (10 mL) was added over the pyridine solution. After a few days, a fine black-red crystalline precipitate was obtained. $C_{26}H_{26}FeN_4O_4 \cdot 2C_5H_5N$ (672.55): calcd. C 64.3, H 5.4, N 12.5; found C 64.4, H 5.2, N 12.4.

$[Fe3(Py)_2]PF_6$: Fe3I (30 mg) was dissolved in pyridine (15 mL) and then a solution of NH_4PF_6 in methanol (2 M) was added dropwise until a precipitate was obtained. $C_{26}H_{26}FeN_4O_4 \cdot 2C_5H_5N \cdot PF_6$ (817.52): calcd. C 52.9, H 4.4, N 10.3; found C 52.8, H 4.6, N 10.1. MS (DEI): *m*/*z* (%) = 79 (100) [pyridine], 514 (<1) [M^+(**Fe3**)].

$[Fe1(Py)_2]PF_6$: Fe1I (30 mg) was dissolved in a solution of pyridine in benzene (1 M, 15 mL) and then a solution of NH_4PF_6 in methanol (2 M) was added dropwise to the solution until a precipitate was obtained. $C_{18}H_{26}FeN_4O_4 \cdot 2C_5H_5N \cdot PF_6$ (721.44): calcd. C 46.6, H 5.0, N 11.7; found C 46.6, H 4.9, N 11.5. MS (DEI): *m*/*z* (%) = 79 (100) [pyridine], 418 (19) [M^+(**Fe1**)].

$[Fe1(N\text{-}MeIm)_2]ClO_4(H_2O)$: Fe1I (30 mg) was dissolved in a solution of *N*-methylimidazole in methanol (1.4 M, 15 mL). A solution of $NaClO_4$ in water was added dropwise to the solution until a precipitate was obtained. $C_{18}H_{26}FeN_4O_4 \cdot 2C_4H_6N_2 \cdot ClO_4 \cdot H_2O$ (693.90): calcd. C 44.6, H 5.7, N 16.0; found C 61.4, H 5.9, N 13.5. MS (DEI): *m*/*z* (%) = 82 (100) [*N*-methylimidazole], 418 (25) [M^+(**Fe1**)].

$Na[Fe2(NO_2)_2](MeOH)_2(H_2O)_{0.5}$: Fe2Cl (0.032 g, 0.05 mmol) was suspended in methanol (5 mL). A solution of sodium nitrite in methanol/water (1 M, 5 mL) was then added. After a few days, black crystals were obtained. The product was collected, washed with a little methanol and dried in vacuo. Yield: 0.01 g (40%). IR (Nujol): $\nu_{C=O}$ = 1665 cm^{-1}. MS (ESI neg.): *m*/*z* (%) = 512 (100) [M^-(**$Fe2NO_2$**)], 558.1 (50) [M^-{**$Fe2(NO_2)_2$**}].

The following procedures were carried out only with the aim of obtaining crystals suitable for X-ray investigations. No yield is given and the main product in the solution may have another identity. Crystal growth was accomplished by using a temperature gradient or different solubility in different solvents. The choice of the counterion may be crucial for crystallisation of the compound. Dropwise addition of nonpolar solvents (*n*-heptane and *n*-hexane are not suitable) can also be used for crystallisation. The addition of water may be used as a last alternative in the case of water-miscible solvents.

$(BzEt_3N)[Fe1(SCN)_2]$: Fe1I (30 mg) was dissolved in 15 mL of a saturated solution of $(BzEt_3N)SCN$ in water/methanol (1:1).

$Et_4N[Fe2(CN)_2](H_2O)_{0.5}$: Fe2I (30 mg) was dissolved in a saturated solution of Et_4NCN in water (15 mL). The mixture was heated and filtered while still hot.

$[Fe2(NO_2)OH_2](MeOH)$: Fe2I (30 mg) was dissolved in methanol (15 mL). The solution was added dropwise to a heated saturated solution of nBu_4NNO_2 in water/methanol (4:1).

$(nBu_4N)_2[Fe3(NO_2)NO_x](NO_2)(H_2O)$: Fe3I (40 mg) was dissolved in dichloromethane (30 mL) and 5 mL of this solution was added to a saturated solution of nBu_4NNO_2 in methanol.

Crystal Structure Determination: The intensity data for the compounds were collected with a Nonius KappaCCD diffractometer, using graphite-monochromated Mo-K_α radiation. Data were corrected for Lorentz and polarisation effects, but not for absorption.[48a,48b] The structures were solved by direct methods (SHELXS[49]) and refined by full-matrix least-squares techniques against F_o^2 (SHELXL-97[50]). The hydrogen atoms were included at calculated positions with fixed thermal parameters. All non-hydrogen atoms were refined anisotropically.[50] Na[**$Fe2(NO_2)_2$**]$(MeOH)_2(H_2O)_{0.5}$ shows a disordered methanol and water molecule with the same oxygen position. This disorder could be solved. The data for compound **Fe1Cl** are not of adequate quality, although the esd's are good enough to be discussed in this paper. For **Fe2**, $[Fe3(Py)_2]PF_6$ and $(nBu_4N)_2$[**$Fe3(NO_2)NO_x$**]$(NO_2)(H_2O)$ we are only publishing the conformation of the central complex unit and the crystallographic data; we will not deposit the data with the Cambridge Crystallographic Data Centre. XP (SIEMENS Analytical X-ray Instruments, Inc.) was used for structure representations.

Crystal Data for Fe1:[51] $C_{18}H_{26}FeN_4O_4$, M_r = 418.28 g mol^{-1}, brown prism, size 0.32×0.20×0.12 mm, monoclinic, space group $P2_1/c$, a = 12.5031(4), b = 11.0732(4), c = 27.4969(6) Å, β = 92.798(2)°, V = 3802.4(2) $Å^3$, T = –90 °C, Z = 8, $\rho_{calcd.}$ =

1.461 g cm^{-3}, μ(Mo-K_α) = 8.25 cm^{-1}, F(000) = 1760, 11872 reflections in h(–16/16), k(–14/13), l(–34/33), measured in the range 1.63° $\leq \theta \leq$ 27.47°, completeness for θ_{max} 90.8%, 7906 independent reflections, R_{int} = 0.028, 5880 reflections with $F_o > 4\sigma(F_o)$, 508 parameters, 0 restraints, $R1_{obs}$ = 0.050, wR^2_{obs} = 0.127, $R1_{all}$ = 0.075, wR^2_{all} = 0.142, GOOF = 0.988, largest difference peak/hole: 0.446/–0.409 e Å^{-3}.

Crystal Data for Fe1MeOH:[51] $C_{19}H_{30}FeN_4O_5$, M_r = 450.32 g mol^{-1}, brown prism, size 0.10 × 0.09 × 0.08 mm, monoclinic, space group $P2_1/n$, a = 7.3249(2), b = 29.5441(9), c = 9.7511(3) Å, β = 94.912(2)°, V = 2102.46(11) Å^3, T = –90 °C, Z = 4, $\rho_{calcd.}$ = 1.423 g cm^{-3}, μ(Mo-K_α) = 7.55 cm^{-1}, F(000) = 952, 8074 reflections in h(–9/9), k(–38/38), l(–12/12), measured in the range 2.76° $\leq \theta \leq$ 27.49°, completeness for θ_{max} 97.2%, 4694 independent reflections, R_{int} = 0.033, 3559 reflections with $F_o > 4\sigma(F_o)$, 271 parameters, 0 restraints, $R1_{obs}$ = 0.038, wR^2_{obs} = 0.093, $R1_{all}$ = 0.060, wR^2_{all} = 0.105, GOOF = 0.838, largest difference peak/hole: 0.349/–0.283 e Å^{-3}.

Crystal Data for Fe2: $C_{22}H_{26}FeN_4O_4$, triclinic, space group $P\bar{1}$, a = 13.019(3), b = 13.753(3), c = 13.757(3) Å, α = 103.28(3), β = 117.00(3), γ = 97.04(3)°, V = 2061.7(8) Å^3, T = –90 °C, Z = 4, F(000) = 976, 5550 measured reflections, 5192 independent reflections, R_{int} = 0.045, 3598 reflections with $I > 2\sigma(I)$, 535 parameters, 0 restraints, $R1$ = 0.162, wR^2 = 0.338, GOOF = 1.052, largest residual electron density: 1.129 e Å^{-3}. Due to technical problems, the measurement stopped too early and reflections at high θ angles are missing. Therefore, the anisotropy refinement and hydrogen atoms were set aside resulting in a dissatisfactory $R1$ value and a high remaining maximum electron density.

Crystal Data for Fe1Cl:[51] $C_{18}H_{26}ClFeN_4O_4$, M_r = 453.73 g mol^{-1}, brown prism, size 0.20 × 0.18 × 0.12 mm^3, monoclinic, space group $P2_1/n$, a = 13.5466(6), b = 7.8215(4), c = 18.5515(9) Å, β = 96.539(3)°, V = 1952.83(16) Å^3, T = –90 °C, Z = 4, $\rho_{calcd.}$ = 1.543 g cm^{-3}, μ(Mo-K_α) = 9.42 cm^{-1}, F(000) = 948, 7129 reflections in h(–17/15), k(–10/9), l(–23/24), measured in the range 3.42° $\leq \theta \leq$ 27.52°, completeness for θ_{max} 96.2%, 4320 independent reflections, R_{int} = 0.065, 3701 reflections with $F_o > 4\sigma(F_o)$, 257 parameters, 0 restraints, $R1_{obs}$ = 0.130, wR^2_{obs} = 0.207, $R1_{all}$ = 0.156, wR^2_{all} = 0.216, GOOF = 1.248, largest difference peak and hole: 1.009/–1.123 e Å^{-3}.

Crystal Data for Fe3(Py)$_2$:[51] $C_{36}H_{36}FeN_6O_4$, triclinic, space group $P\bar{1}$, a = 10.6327(3), b = 12.0421(4), c = 14.7871(5) Å, α = 66.015(2), β = 71.582(2), γ = 66.368(2)°, V = 1558.09(9) Å^3, T = –90 °C, Z = 2, F(000) = 704, 12217 measured reflections, 7108 independent reflections, R_{int} = 0.028, 6385 reflections with $I > 2\sigma(I)$, 424 parameters, 0 restraints, $R1$ = 0.044, wR^2 = 0.103, GOOF = 1.016, largest residual electron density: 0.421 e Å^{-3}.

Crystal Data for [Fe3(Py)$_2$]PF$_6$: $C_{36}H_{36}F_6FeN_6O_4P$, orthorhombic, space group $Pbca$, a = 16.840(3), b = 20.335(4), c = 20.857(4) Å, V = 7142(3) Å^3, T = –90 °C, Z = 8, μ(Mo-K_α) = 5.65 cm^{-1}, F(000) = 3368. The data are not of the best quality and so we are publishing only the conformation of the molecule, although the distances and angles are of plausible size.

Crystal Data for [Fe1(Py)$_2$]PF$_6$:[51] $C_{28}H_{36}F_6FeN_6O_4P$, monoclinic, space group $P2_1/n$, a = 9.211(2), b = 14.861(3), c = 24.180(5) Å, β = 100.51(3)°, V = 3254.2(11) Å^3, T = 20 °C, Z = 4, F(000) = 1492, 8631 measured reflections, 4697 independent reflections, R_{int} = 0.028, 3596 reflections with $I > 2\sigma(I)$, 442 parameters, 0 restraints, $R1$ = 0.052, wR^2 = 0.138, GOOF = 1.067, largest residual electron density: 0.436 e Å^{-3}.

Crystal Data for [Fe1(N-MeIm)$_2$]ClO$_4$(H$_2$O):[51] $C_{26}H_{40}ClFeN_8O_9$, monoclinic, space group $P2_1/n$, a = 14.897(1), b = 13.613(1), c = 16.096(1) Å, β = 95.950(7)°, V = 3246.6(4) Å^3, T = –90 °C, Z = 4, F(000) = 1468, 12274 measured reflections, 7233 independent reflections, R_{int} = 0.082, 4759 reflections with $I > 2\sigma(I)$, 425 parameters, 0 restraints, $R1$ = 0.131, wR^2 = 0.238, GOOF = 1.140, largest residual electron density: 0.552 e Å^{-3}.

Crystal Data for (BzEt$_3$N)[Fe1(NCS)$_2$]:[51] $C_{33}H_{48}FeN_7O_4S_2$, monoclinic, space group $P2_1/n$, a = 11.7266(2), b = 24.7177(6), c = 12.7940(2) Å, β = 96.551(1)°, V = 3684.19(12) Å^3, T = –90 °C, Z = 4, F(000) = 1540, 7450 measured reflections, 7450 independent reflections, 5659 reflections with $I > 2\sigma(I)$, 487 parameters, 0 restraints, $R1$ = 0.056, wR^2 = 0.118, GOOF = 1.055, largest residual electron density: 0.415 e Å^{-3}.

Crystal Data for Et$_4$N[Fe2(CN)$_2$](H$_2$O):[51] $C_{32}H_{48}FeN_7O_5$, monoclinic, space group $P2_1/n$, a = 11.1860(2), b = 11.8490(4), c = 25.0733(9) Å, β = 92.355(2)°, V = 3320.5(5) Å^3, T = –90 °C, Z = 4, F(000) = 1420, 13220 measured reflections, 7482 independent reflections, R_{int} = 0.062, 4899 reflections with $I > 2\sigma(I)$, 446 parameters, 0 restraints, $R1$ = 0.063, wR^2 = 0.119, GOOF = 1.010, largest residual electron density: 0.436 e Å^{-3}.

Crystal Data for [Fe2(NO$_2$)OH$_2$](MeOH):[51] $C_{23}H_{29}FeN_6O_{10}$, orthorhombic, space group $Pna2_1$, a = 16.273(1), b = 11.6454(7), c = 13.8026(7) Å, V = 2615.7(3) Å^3, T = –90 °C, Z = 4, F(000) = 1180, 5725 measured reflections, 5725 independent reflections, 4004 reflections with $I > 2\sigma(I)$, 344 parameters, 1 restraint (origin of the unit cell), $R1$ = 0.077, wR^2 = 0.138, GOOF = 1.031, largest residual electron density: 0.507 e Å^{-3}.

Crystal Data for Na[Fe2(NO$_2$)$_2$](MeOH)$_2$(H$_2$O)$_{0.5}$:[51] $C_{46.4}H_{67.2}Fe_2N_{12}Na_2O_{22}(CH_4O)_2$, M_r = 1366.89 g mol^{-1}, red-brown prism, size 0.12 × 0.10 × 0.09 mm, monoclinic, space group $P2_1/n$, a = 11.3381(3), b = 13.3795(6), c = 21.1046(8) Å, β = 102.522(2)°, V = 3125.4(2) Å^3, T = –90 °C, Z = 2, $\rho_{calcd.}$ = 1.452 g cm^{-3}, μ(Mo-K_α) = 5.65 cm^{-1}, F(000) = 1431, 11116 reflections in h(–14/14), k(–14/17), l(–27/27), measured in the range 1.89° $\leq \theta \leq$ 27.48°, completeness for θ_{max} 98.8%, 7082 independent reflections, R_{int} = 0.033, 5071 reflections with $F_o > 4\sigma(F_o)$, 419 parameters, 0 restraints, $R1_{obs}$ = 0.0546, wR^2_{obs} = 0.1280, $R1_{all}$ = 0.0886, wR^2_{all} = 0.146, GOOF = 0.962, largest difference peak/hole: 0.845/–0.619 e Å^{-3}.

Crystal Data for (nBu$_4$N)$_2$[Fe3(NO$_2$)NO$_x$](NO$_2$)(H$_2$O): $C_{58}H_{100}FeN_9O_{11}$ (x = 2), M_r = 1161.32 g mol^{-1}, green prism, size 0.34 × 0.32 × 0.20 mm, triclinic, space group $P\bar{1}$, a = 12.961(3), b = 15.203(4), c = 17.985(4) Å, α = 94.779(9), β = 106.047(9), γ = 107.84(1)°, V = 3186.9(13) Å^3, T = –90 °C, measured in the range 3.03° $\leq \theta \leq$ 27.59°.

Crystal Data for (Fe1)$_2$dabco:[51] $C_{42}H_{64}Fe_2N_{10}O_8$, M_r = 948.73 g mol^{-1}, brown prism, size 0.10 × 0.09 × 0.08 mm, triclinic, space group $P\bar{1}$, a = 8.3623(2), b = 11.8244(3), c = 12.6364(3) Å, α = 110.604(2), β = 100.490(2), γ = 100.238(2)°, V = 1109.61(5) Å^3, T = –90 °C, Z = 1, $\rho_{calcd.}$ = 1.420 g cm^{-3}, μ(Mo-K_α) = 7.17 cm^{-1}, F(000) = 502, 8736 reflections in h(–10/10), k(–14/15), l(–16/16), measured in the range 2.03° $\leq \theta \leq$ 27.46°, completeness for θ_{max} 99.6%, 5057 independent reflections, R_{int} = 0.0221, 4346 reflections with $F_o > 4\sigma(F_o)$, 307 parameters, 0 restraints, $R1_{obs}$ = 0.0490, wR^2_{obs} = 0.1398, $R1_{all}$ = 0.0586, wR^2_{all} = 0.1478, GOOF = 1.018, largest difference peak/hole: 1.059/–0.673 e Å^{-3}.

Crystal Data for (Fe2)$_2$dabco:[51] $C_{50}H_{64}Fe_2N_{10}O_8$, M_r = 1044.81 g mol^{-1}, black prism, size 0.10 × 0.09 × 0.08 mm, monoclinic, space group $P2_1/n$, a = 11.8119(2), b = 13.1486(3), c = 16.7867(3) Å, α = 90.00, β = 108.6320(10), γ = 90.00°, V = 2470.50(8) Å^3, T = –90 °C, Z = 2, $\rho_{calcd.}$ = 1.405 g cm^{-3}, μ(Mo-K_α) = 6.52 cm^{-1}, F(000) = 1100, 18857 reflections in h(–14/15), k(–17/

17), *l*(–21/20), measured in the range 2.39° ≤ θ ≤ 27.47°, completeness for θ_{max} 99.8%, 5644 independent reflections, R_{int} = 0.0422, 4402 reflections with $F_o > 4\sigma(F_o)$, 308 parameters, 0 restraints, $R1_{obs}$ = 0.0516, wR^2_{obs} = 0.1412, $R1_{all}$ = 0.0710, wR^2_{all} = 0.1535, GOOF = 1.026, largest difference peak/hole: 1.094/–0.833 e Å^{-3}.

Crystal Data for (Fe3)$_2$dabco:[51] $C_{58}H_{64}Fe_2N_{10}O_8{\cdot}CH_3OH$, M_r = 1172.93 g mol^{-1}, dark-green prism, size 0.10 × 0.09 × 0.08 mm, triclinic, space group $P\bar{1}$, a = 11.3944(6), b = 12.2186(8), c = 13.1020(8) Å, α = 116.067(4), β = 113.938(3), γ = 93.166(4)°, V = 1435.76(15) Å^3, T = –90 °C, Z = 1, $\rho_{calcd.}$ = 1.357 g cm^{-3}, μ(Mo-K_α) = 5.7 cm^{-1}, F(000) = 616, 10088 reflections in *h*(–14/14), *k*(–15/14), *l*(–16/16), measured in the range 2.04° ≤ θ ≤ 27.40°, completeness for θ_{max} 98.3%, 6431 independent reflections, R_{int} = 0.0396, 5119 reflections with $F_o > 4\sigma(F_o)$, 387 parameters, 0 restraints, $R1_{obs}$ = 0.1018, wR^2_{obs} = 0.2585, $R1_{all}$ = 0.1240, wR^2_{all} = 0.2702, GOOF = 1.160, largest difference peak/hole: 1.090/–0.734 e Å^{-3}.

Acknowledgments

We gratefully acknowledge financial support from the Deutsche Forschungsgemeinschaft and the Fonds der Chemischen Industrie. The authors thank Dr. V. Schünemann and P. Wegner (Lübeck) for the Mössbauer spectrum, Dr. W. Poppitz and S. Schönau for the MS measurements, Dr. M. Friedrich and B. Rambach for measuring the ESR spectra, and Dr. K. Karaghiosoff for measuring the ^{1}H NMR spectrum of **Fe1Cl**.

[1] W. Kaim, B. Schwederski, "Bioinorganic Chemistry: Inorganic Elements", in *The Chemistry of Life*, John Wiley & Sons, Chichester, **1994.**

[2] *The Porphyrin Handbook* (Eds.: K. M. Kadish, K. M. Smith, R. Guilard), Elsevier–Academic Press, **1999**, vol. 1–10 and **2003**, vol. 11–20.

[3] T. Tsumaki, *Bull. Chem. Soc. Jpn.* **1938**, *13*, 252.

[4] a) E. N. Jacobsen, *Comprehensive Organometallic Chemistry II* (Eds.: G. Wilkinson, F. G. A. Stone, E. W. Abel, L. S. Hegedus), Pergamon, New York, **1995**, vol. 12 chapter 11.1; b) T. Katsuki, *Coord. Chem. Rev.* **1995**, *140*, 189.

[5] a) E.-G. Jäger, in *Chemistry at the Beginning of the Third Millennium* (Eds.: L. Fabbrizzi, A. Poggi), Springer-Verlag, Berlin, Heidelberg, New York, **2000**, p. 103; b) E.-G. Jäger, J. Knaudt, K. Schuhmann, A. Guba, in *Peroxide Chemistry – Mechanistic and Preparative Aspects of Oxygen Transfer* (Ed.: W. Adam), Wiley-VCH, Weinheim, **2000**, p. 249; c) E.-G. Jäger, St. Barth, H. Keutel, F. Wiesemann, U. Gaudig, in *Bioinorganic Chemistry – Transition Metals in Biology and their Coordination Chemistry* (Ed.: A. X. Trautwein), Wiley-VCH, Weinheim, **1997**, p. 584.

[6] a) E.-G. Jäger, *Z. Anorg. Allg. Chem.* **1969**, *364*, 177; b) E.-G. Jäger, *Z. Chem.* **1964**, *4*, 437.

[7] a) P. Mountford, *Chem. Soc. Rev.* **1998**, *27*, 105; b) F. A. Cotton, J. Czuchajowska, *Polyhedron* **1990**, *9*, 2553.

[8] a) R. Wegner, M. Gottschaldt, H. Görls, E.-G. Jäger, D. Klemm, *Chem. Eur. J.* **2001**, *7*, 2143; *Angew. Chem.* **2000**, *112*, 608; *Angew. Chem. Int. Ed.* **2000**, *39*, 595; b) H. Keutel, H. Görls, W. Poppitz, A. Schütz, E.-G. Jäger, *J. Prakt. Chem.* **1999**, *341*, 785; c) H. Elias, D. Hess, H. Paulus, E.-G. Jäger, F. Gräfe, *Z. Anorg. Allg. Chem.* **1990**, *101*, 101; d) E.-G. Jäger, K. Müller, *Z. Anorg. Allg. Chem.* **1985**, *526*, 29; e) E.-G. Jäger, K. Müller, *Z. Anorg. Allg. Chem.* **1981**, *482*, 201.

[9] a) Y. Nishida, K. Hayashida, N. Oishi, S. Kida, *Inorg. Chim. Acta* **1980**, *38*, 213; b) V. V. Minin, Yu. V. Rakitin, G. M. Larin, E.-G. Jäger, *Zh. Neorg. Khim.* **1981**, *26*, 650; *Chem. Abstr.* **1981**, *94*, 200292z.

[10] a) D. G. Pillsbury, D. H. Busch, *J. Am. Chem. Soc.* **1976**, *98*, 7836; b) J. A. Streeky, D. G. Pillsbury, D. H. Busch, *Inorg. Chem.* **1980**, *19*, 3148; c) Yu. E. Kovalenko, Ya. D. Lampeka, I. Ya. Levitin, K. B. Yatsimirkii, K. Müller, D. Seidel, E.-G. Jäger, *Russ. Chem. Bull.* **1993**, *42*, 981 (Engl. Transl. from *Izv. Akad. Nauk Ser. Khim.* **1993**, no. 6, 1092); d) E.-G. Jäger, H. Keutel, M. Rudolph, B. Krebs, F. Wiesemann, *Chem. Ber.* **1995**, *128*, 503.

[11] a) E.-G. Jäger, M. Rudolph, R. Müller, *Z. Chem.* **1978**, *18*, 229; b) E.-G. Jäger, P. Renner, R. Schmidt, *Z. Chem.* **1978**, *18*, 193; c) E.-G. Jäger, B. Kirchhof, E. Schmidt, B. Remde, A. Kipke, R. Müller, *Z. Anorg. Allg. Chem.* **1982**, *485*, 141; d) E.-G. Jäger, G. Schlenvoigt, B. Kirchhof, M. Rudolph, R. Müller, *Z. Anorg. Allg. Chem.* **1982**, *485*, 173; e) E.-G. Jäger, K. Schuhmann, H. Görls, *Inorg. Chim. Acta* **1997**, *255*, 295; E.-G. Jäger, K. Schuhmann, H. Görls, *Chem. Ber./Recueil* **1997**, *130*, 1643; f) K. Schuhmann, E.-G. Jäger, *Eur. J. Inorg. Chem.* **1998**, 2051.

[12] a) K. Kubokura, H. Okawa, S. Kida, *Bull. Chem. Soc. Jpn.* **1978**, *51*, 2036; b) G. M. Larin, V. V. Minin, E.-G. Jäger, P. Renner, *Zh. Neorg. Khim.* **1980**, *25*, 183; *Chem. Abstr.* **1980**, *92*, 139940z; c) E.-G. Jäger, K. Müller, *Z. Anorg. Allg. Chem.* **1983**, *501*, 40; d) E.-G. Jäger, J. Knaudt, M. Rudolph, M. Rost, *Chem. Ber.* **1996**, *129*, 1041; e) J. Knaudt, St. Förster, U. Bartsch, A. Rieker, E.-G. Jäger, *Z. Naturforsch., Teil B* **2000**, *55*, 86; f) R. Wegner, M. Gottschaldt, W. Poppitz, E.-G. Jäger, D. Klemm, *J. Mol. Catal. A: Chem.* **2003**, *201*, 91.

[13] M. Rudolph, S. Dautz, E.-G. Jäger, *J. Am. Chem. Soc.* **2000**, *122*, 10821.

[14] a) E.-G. Jäger, D. Seidel, M. Rudolph, A. Schneider, *Z. Chem.* **1986**, *26*, 76; b) H. Görls, G. Reck, E.-G. Jäger, K. Müller, D. Seidel, *Cryst. Res. Technol.* **1990**, *25*, 1277.

[15] a) D. P. Riley, J. A. Stone, D. H. Busch, *J. Am. Chem. Soc.* **1977**, *99*, 767; b) D. P. Riley, D. H. Busch, *Inorg. Chem.* **1984**, *23*, 3235; c) T. J. Truex, R. H. Holm, *J. Am. Chem. Soc.* **1972**, *94*, 4529; d) S. Koch, R. H. Holm, R. B. Frankel, *J. Am. Chem. Soc.* **1975**, *97*, 6714.

[16] a) V. L. Goedken, J. J. Pluth, S.-M. Peng, B. Bursten, *J. Am. Chem. Soc.* **1976**, *98*, 8014; b) M. C. Weiss, B. Bursten, S.-M. Peng, V. L. Goedken, *J. Am. Chem. Soc.* **1976**, *98*, 8021; c) V. L. Goedken, S. M. Peng, J. Molin-Norris, Y. Park, *J. Am. Chem. Soc.* **1976**, *98*, 8391; d) V. L. Goedken, Y.-A. Park, *J. Chem. Soc., Chem. Commun.* **1975**, 214.

[17] a) E.-G. Jäger, *Vortragsberichte zum Symposium "Koordinationschemie der Übergangselemente"*, Sektion C, Jena **1969**, p. 96; b) E.-G. Jäger, E. Stein, F. Gräfe, W. Schade, *Z. Anorg. Allg. Chem.* **1985**, *526*, 15; c) E.-G. Jäger, F. Gräfe, *Z. Anorg. Allg. Chem.* **1988**, *561*, 25.

[18] a) F. Wiesemann, R. Wonnemann, B. Krebs, H. Keutel, E.-G. Jäger, *Angew. Chem. Int. Ed. Engl.* **1994**, *33*, 1363; b) I. Käpplinger, H. Keutel, E.-G. Jäger, *Inorg. Chim. Acta* **1999**, *291*, 190; c) I. Käpplinger, M. Grodzicki, V. Schünemann, H. Görls, A. X. Trautwein, E.-G. Jäger, private communication, Cambridge Crystallographic Data Centre, CSD 408794/5, October **1998**.

[19] a) E.-G. Jäger, *Z. Chem.* **1985**, *25*, 446; b) E.-G. Jäger, B. Schweder, S. Radzuweit, *Z. Chem.* **1988**, *28*, 152; c) E.-G. Jäger, H. Keutel, *Inorg. Chem.* **1997**, *36*, 3512.

[20] H. Keutel, I. Käpplinger, E.-G. Jäger, M. Grodzicki, V. Schünemann, A. X. Trautwein, *Inorg. Chem.* **1999**, *38*, 2320.

[21] E.-G. Jäger, H. Hähnel, H.-F. Klein, A. Schmidt, *J. Prakt. Chem.* **1991**, *333*, 423.

[22] a) B. Weber, H. Görls, M. Rudolf, E.-G. Jäger, *Inorg. Chim. Acta* **2002**, *337*, 247; b) B. Weber, PhD Thesis, University of Jena, **2002**; c) B. Weber, *A Contribution to a Deeper Understanding of the Nature of the Iron–Nitrosyl Bond in Bioanalogue Iron Complexes*, Der Andere Verlag, Osnabrück, **2003**.

[23] a) K. Müller, E.-G. Jäger, *Z. Anorg. Allg. Chem.* **1989**, *577*, 195; b) E.-G. Jäger, D. Seidel, W. Schade, *Z. Chem.* **1983**, *23*, 32; c) E.-G. Jäger, D. Seidel, *Z. Chem.* **1983**, *23*, 261; d) W. Schade, E.-G. Jäger, K. Müller, D. Seidel, *J. Prakt. Chem.* **1989**, *331*, 559.

[24] a) O. K. Medhi, J. Silver, *J. Chem. Soc., Chem. Commun.* **1989**, 1199; b) A. Hudson, H. J. Whitfield, *Inorg. Chem.* **1967**, *6*, 1120.
[25] A. Walker, *Proton NMR and EPR spectroscopy of Paramagnetic Metalloporphyrins*, in *The Porphyrin Handbook* (Eds.: K. M. Kadish, K. M. Smith, R. Guilard), **2000**, Vol. 5, Ch. 36, p. 81.
[26] K. R. Levan, C. E. Strouse, *Abstract of paper, American Crystallographic Association Summer meeting*, Snowman, **1983**.
[27] a) E. Elkaim, K. Tanaka, P. Coppens, W. R. Scheidt, *Acta Crystallogr., Sect. B.* **1987**, *43*; 457; b) D. K. Geiger, Y. J. Lee, W. R. Scheidt, *J. Am. Chem. Soc.* **1984**, *106*, 6339.
[28] W. R. Scheidt, Y. J. Lee, *Struct. Bonding (Berlin)* **1987**, *64*, 1.
[29] *Nitric Oxide. Principles and Actions* (Ed.: J. Lancaster), Academic Press, San Diego, **1996**.
[30] P. L. Feldman, O. W. Griffith, D. J. Stuehr, *Chem. Eng. News* **1993**, *71*, 26.
[31] O. Einsle, A. Messerschmidt, P. Stach, G. P. Bourenkov, H. D. Bartunik, R. Huber, P. M. H. Kroneck, *Nature* **1999**, *400*, 476.
[32] a) H. Nasri, J. A. Goodwin, W. R. Scheidt, *Inorg. Chem.* **1990**, *29*, 185; b) H. Nasri, Y. Wang, B. H. Huynh, A. F. Walker, W. R. Scheidt, *Inorg. Chem.* **1991**, *30*, 1483; c) H. Nasri, K. J. Haller, Y. Wang, B. H. Huynh, W. R. Scheidt, *Inorg. Chem.* **1992**, *31*, 3459; d) M. K. Ellison, C. E. Schulz, W. R. Scheidt, *Inorg. Chem.* **1999**, *38*, 100; e) H. Nasri, M. K. Ellison, S. Chen, B. H. Huynh, W. R. Scheidt, *J. Am. Chem. Soc.* **1997**, *119*, 6724.
[33] L. Wolf, E.-G. Jäger, *Z. Anorg. Allg. Chem.* **1966**, *346*, 76.
[34] a) A. R. Newman, A. N. French, *Inorg. Chim. Acta* **1987**, *129*, L37; b) M. G. Finnegan, A. G. Lappin, W. R. Scheidt, *Inorg. Chem.* **1990**, *29*, 181; c) M. Frangione, J. Port, M. Baldiwala, A. Judd, J. Galley, M. DeVega, K. Linna, L. Caron, E. Anderson, J. A. Goodwin, *Inorg. Chem.* **1997**, *36*, 1904.
[35] a) T. Ikeue, Y. Ohgo, T. Yamaguchi, M. Takahashi, M. Takeda, M. Nakamura, *Angew. Chem. Int. Ed.* **2001**, *40*, 2617; b) W. O. Koch, V. Schünemann, M. Gerdan, A. X. Trautwein, H.-J. Krüger, *Chem. Eur. J.* **1998**, *4*, 686; c) F. V. Wells, S. W. McCann, H. H. Wickman, S. L. Kessel, D. N. Hendrickson, R. D. Feltham, *Inorg. Chem.* **1982**, *21*, 2306; d) E. König, G. Ritter, J. Dengler, L. F. Larkworthy, *Inorg. Chem.* **1992**, *31*, 1196.
[36] P. Gütlich, A. Hauser, H. Spiering, *Angew. Chem.* **1994**, *106*, 2109; *Angew. Chem. Int. Ed. Engl.* **1994**, *33*, 2024.
[37] a) M. Mylrajan, L. A. Andersson, J. Sun, T. M. Loer, C. S. Thomas, E. P. Sullivan Jr., M. A. Thomson, K. M. Long, O. P. Anderson, S. H. Strauss, *Inorg. Chem.* **1995**, *34*, 3953; b) H. Nasri, M. Debbabi, *Polyhedron* **1998**, *17*, 3607.
[38] a) W. R. Scheidt, Y. J. Lee, D. K. Geiger, K. Taylor, K. Hatano, *J. Am. Chem. Soc.* **1982**, *104*, 3367; b) D. K. Geiger, V. Chumplang, W. R. Scheidt, *Inorg. Chem.* **1985**, *24*, 4736.
[39] a) M. J. Maroney, E. O. Fey, D. A. Baldwin, R. E. Stenkamp, L. H. Jensen, N. J. Rose, *Inorg. Chem.* **1986**, *25*, 1409; b) L. Ballester, A. Gutierrez, M. F. Perpinan, S. Rico, M. T. Azcondo, C. Belletto, *Inorg. Chem.* **1999**, *38*, 4430.
[40] I. Käpplinger, PhD Thesis, University of Jena, **2002**.
[41] a) W. R. Scheidt, K. J. Haller, K. Hatano, *J. Am. Chem. Soc.* **1980**, *102*, 3017; b) M. Schappacher, J. Fischer, R. Weiss, *Inorg. Chem.* **1989**, *28*, 389; c) T. J. Bartczak, S. Wolowiec, L. Latos-Grazynski, *Inorg. Chim. Acta* **1998**, *277*, 242.
[42] M. Nakamura, T. Ikeue, H. Fujii, T. Toshimura, *J. Am. Chem. Soc.* **1997**, *119*, 6284.
[43] Autorenkollektiv, *Organikum*, Johann Ambrosius Barth Verlagsgesellschaft mbH, Leipzig, Berlin, Heidelberg, **1993**.
[44] M. Grodzicki, *J. Phys. B* **1980**, *13*, 2683.
[45] M. Grodzicki, "Theory and Application of the Self-Consistent-Charge Xα Method", habilitation thesis, Hamburg, Germany, **1985**.
[46] a) E.-G. Jäger, *Z. Chem.* **1968**, *8*, 30; b) E.-G. Jäger, *Z. Chem.* **1968**, *8*, 470.
[47] L. Claisen, *Justus Liebigs Ann. Chem.* **1897**, *279*, 1.
[48] a) *COLLECT, Data Collection Software*, B. V. Nonius, The Netherlands, **1998**; b) Z. Otwinowski, W. Minor, *Processing of X-ray Diffraction Data Collected in Oscillation Mode*, in *Methods in Enzymology, Macromolecular Crystallography, Part A* (Eds.: C. W. Carter, R. M. Sweet), Academic Press, San Diego, **1997**, vol. 276, p. 307.
[49] G. M. Sheldrick, *Acta Crystallogr., Sect. A* **1990**, *46*, 467.
[50] G. M. Sheldrick, *SHELXL-97*, University of Göttingen, Germany, **1993**.
[51] CCDC-240934 (**Fe1**), -240945 (**Fe1MeOH**), -240936 (**Fe1Cl**), -240937 {Na[**Fe2(NO$_2$)$_2$**](MeOH)$_2$(H$_2$O)$_{0.5}$}, -241784 [**Fe3(Py)$_2$**], -241781 {[**Fe1(Py)$_2$**]PF$_6$}, -241782 {[**Fe1(N-MeIm)$_2$**]ClO$_4$(H$_2$O)}, -241785 {(BzEt$_3$N)[**Fe1(NCS)$_2$**]}, -241783 {Et$_4$N[**Fe2(CN)$_2$**](H$_2$O)}, -241780 {[**Fe2(NO$_2$)OH$_2$**]MeOH}, -266535 [**(Fe1)$_2$dabco**], -266536 [**(Fe2)$_2$dabco**], and -266537 [**(Fe3)$_2$dabco**·MeOH] contain the supplementary crystallographic data for this paper. These data can be obtained free of charge from The Cambridge Crystallographic Data Centre via www.ccdc.cam.ac.uk/data_request/cif.

Received: September 13, 2004
Published Online: June 14, 2005

